

GEOCHEMISTRY OF VOLCANIC AND SUBVOLCANIC ROCKS AND BIOSTRATIGRAPHY ON RADIOLARIAN CHERTS FROM THE ALMOPIAS OPHIOLITES AND PAIKON UNIT (WESTERN VARDAR, GREECE)

Emilio Saccani*, **Marco Chiari****, **✉**, **Valerio Bortolotti*****, **Adonis Photiades^o** and **Gianfranco Principi*****

* *Dipartimento di Fisica e Scienze della Terra, Università di Ferrara, Italy.*

** *C.N.R., Istituto di Geoscienze e Georisorse, Unità di Firenze, Italy.*

*** *Dipartimento di Scienze della Terra, Università di Firenze, Italy.*

^o *Institute of Geology and Mineral Exploration (IGME), Athens, Greece.*

✉ *Corresponding author, email: mchiari@geo.unifi.it*

Keywords: *ophiolite, geochemistry, biostratigraphy, radiolarian chert, Almopias, Paikon, Triassic, Jurassic. Greece.*

ABSTRACT

The Almopias and Paikon “sub-zones” in northern Greece represent the easternmost part of the Vardar Domain. Volcanic sequences in the Paikon sub-zone largely consist of calc-alkaline volcanic rocks with very minor normal-type (N-) mid-ocean ridge basalts (MORB) and boninites. These data confirm that the Paikon volcanics have originated in a volcanic arc setting developed during the Middle to Late Jurassic times on the westernmost continental margin of the European plate. The Almopias “sub-zone” consists of several ophiolite-bearing tectonic units showing a complex combination of different metamorphic, litho-stratigraphical, and age characteristics. The Liki, Nea Zoi, and Vrissi units (central Almopias) are ophiolitic mélanges, the Mavrolakkos and Krania units (eastern Almopias) consist of volcanic sequences, and the Ano Garefi unit (eastern Almopias) includes serpentinized peridotites and overlying basaltic lavas.

The Liki unit underwent metamorphism and deformation under amphibolite-facies condition and includes rocks showing N-MORB and low-K island arc tholeiitic affinities. The Nea Zoi unit incorporates N-MORBs of unknown age and Late Triassic calc-alkaline rocks. The Vrissi unit includes an incomplete volcanic sequence consisting of MORB-type volcanics cross cut by arc-type dyke and Middle-Late Jurassic arc-type volcanic rocks. The Mavrolakkos unit consists of sheeted dykes, lavas, and individual dykes with N-MORB affinity, which are crosscut by dykes showing volcanic arc affinity. The Krania unit consists of Middle-Late Jurassic N-MORB series tectonically associated with calc-alkaline volcanics and dykes. Basalts of the Ano Garefi unit have alkaline affinity, whereas dikes cutting the peridotites show enriched-type MORB chemistry.

Our data show the occurrence in the Almopias units of Middle-Late Jurassic N-MORB lavas associated with overlying coeval volcanic arc-type lavas and/or intruded by volcanic arc-type dykes. A major point arising from this paper is that some of the Almopias ophiolitic units do not correlate with the other ophiolitic units in the Dinaride-Hellenide belt and some could correlate with the northernmost extension of the Vardar zone in the South Apuseni - Transylvanian ophiolitic belt in Romania.

INTRODUCTION

The Dinaric-Hellenic belt is derived from the Mesozoic to Neogene convergence between the Eurasian and the Adria plates, by a complex geodynamic evolution from continental rifting to oceanic spreading (Middle Triassic to Late Jurassic), subduction and continental collision stages (Late Jurassic/Early Cretaceous up today) (see Bortolotti and Principi, 2005; Dilek et al., 2008; Robertson, 2012; Bortolotti et al., 2013 for a comprehensive review). This long-lived geodynamic evolution produced the present-day structural pattern of the Dinaric-Hellenic belt, represented by an assemblage of northwest-southeast trending tectono-stratigraphic domains (Fig. 1).

Along the Greek transect of the Dinaric-Hellenic belt several tectono-stratigraphic zones or domains have been classically identified in literature (Fig. 1a). According to Bortolotti et al. (2013), the westernmost zones (Pre-Apulian, Ionian, Gavrovo-Tripolitza, Pindos), as well as the Pelagonian zone represent the deformed Adria Continental Domain. The deformed Adria Continental Domain is thrust to the west onto the undeformed Adria zone, today located in the Adriatic Sea (Fig. 1 and Pre-Apulian zone in Fig. 2a). In contrast, Serbo-Macedonian zone-Rhodope Massif represents the eastern margin of the Eurasian Plate. Ophiolites are widespread in the so-called Subpelagonian, Pelagonian and Vardar zones (Fig. 2a).

According to Ferrière et al. (2012) and Bortolotti et al. (2013), the term Subpelagonian zone has to be abandoned as an isopic or ophiolitic zone or as an ocean. It initially referred to the transition between the Pelagonian platform and the Pindos basin (Aubouin, 1959), but was generally used for identifying an oceanic basin located to the west of the Pelagonian platform (see Robertson, 2012). However, many authors do not agree with this interpretation and refer the Subpelagonian and Pelagonian ophiolites to the Vardar Oceanic Domain (e.g., Bortolotti et al., 2013, and bibl. therein). In fact, Chiari et al. (2012) have grouped the Pelagonian and Subpelagonian zones into Pelagonian *sensu lato* tectonic units of the deformed Adria Continental Domain. In order to avoid confusion between actual geographic location of ophiolites and their origin, Saccani et al. (2011) grouped all the Albanide-Hellenide ophiolites into two major ophiolitic belts: 1) the External Ophiolites (now cropping out in the Subpelagonian and Pelagonian zones) and 2) the Internal Ophiolites (cropping out in the Vardar area) (Fig. 2a). Likewise, Ferrière et al. (2012) distinguished a Supra-Pelagonian ophiolitic belt on the west (= External ophiolites) and a Vardarian belt (= Internal ophiolites) on the east.

As already mentioned, there is no general consensus about the geodynamic significance of the External and Internal Ophiolites. According to some authors, the External and Internal Ophiolites represent remnants of the Mirdita-Pindos Ocean and the Vardar Ocean, respectively. These two Neo-Tethys

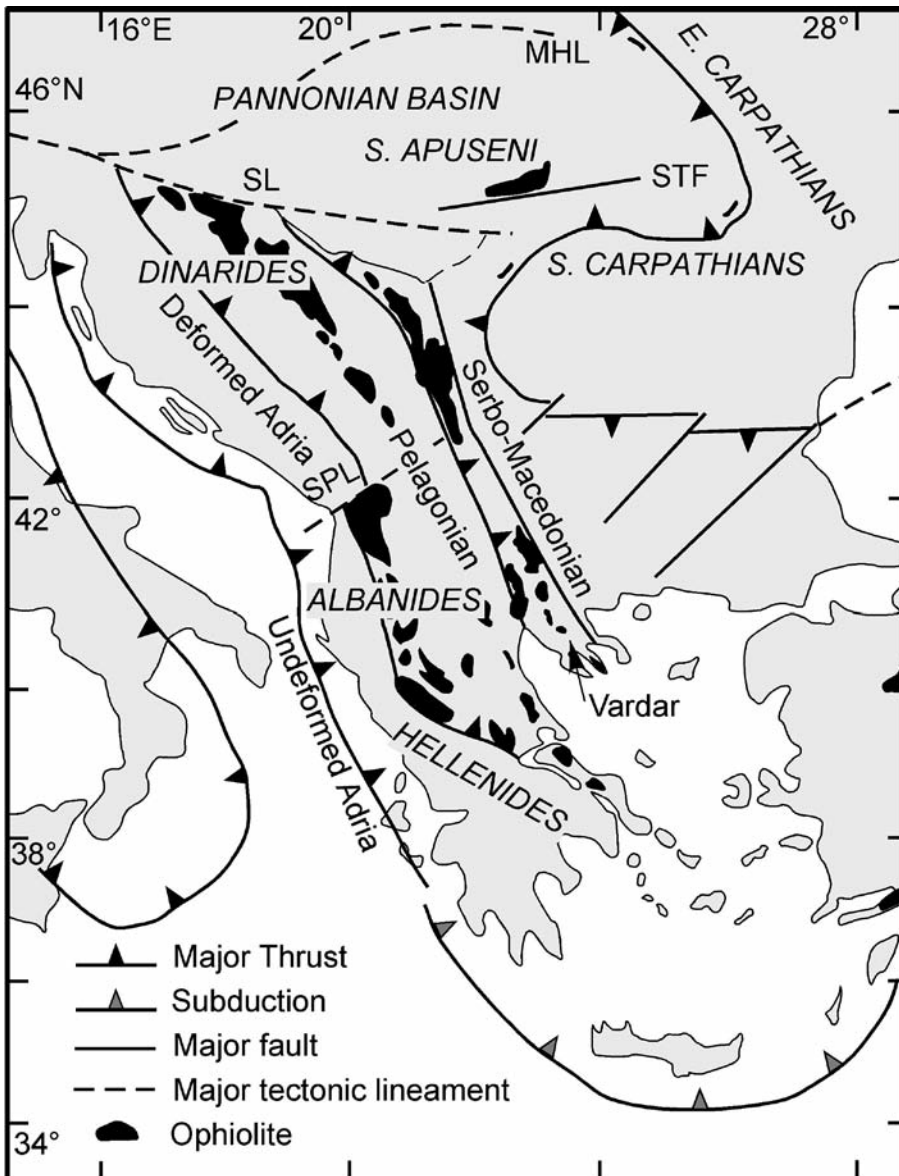


Fig. 1 - Simplified tectonic scheme of the Dinaric-Hellenic belt and surrounding areas. Modified from Bortolotti and Principi (2005). The Pelagonian domain includes the Subpelagonian zone according to Ferrière et al. (2012) and Bortolotti et al. (2013). Abbreviations: MHL- Mid-Hungarian line; STF- South Transylvanian fault; SL- Sava line; SPL- Scutari-Peć line.

oceanic branches were separated by the Pelagonian micro-continental block (e.g., Jones and Robertson, 1991; Shallo et al., 1992; Doutsos et al., 1993; Robertson and Shallo, 2000; Dilek et al., 2007).

In contrast, other authors (e.g., Bernoulli and Laubscher 1972; Vergély, 1976; Çollaku et al., 1992; Schermer, 1993; Bortolotti et al., 1996; 2002b; 2004a; 2013; Schmid et al., 2008; Ferrière et al., 2012; Chiari et al., 2012; 2013) suggested that both External and Internal Ophiolites (except the Guevgueli Complex) represent remnants of a single oceanic basin rooted in the Vardar area and that the Pelagonian domain represented the northernmost edge of the Adria plate. In this paper, we assume an eastern origin for the both External and Internal ophiolites, originated in the Vardar Ocean, located on the eastern side of the Pelagonian margin (and constituting the Vardar Oceanic Domain) and successively thrust westwards, till Mirdita and Pindos areas. Now its terranes represent the uppermost tectonic unit of Hellenides, which the roots now exposed in the East Macedonia immediately west of Thessaloniki.

Based on literature data, the Internal and External Ophiolites show some distinctive features. The External Ophiolites

are characterized by the occurrence of huge and coherent Mid Jurassic crustal sequences formed in both oceanic, subduction unrelated setting and intra-oceanic supra-subduction zone (SSZ) setting, which are lacking in the Internal Ophiolites. In contrast, the Internal Ophiolites are mainly characterized by the occurrence of Late Jurassic back-arc basin sequences associated with calc-alkaline basalts (CAB) cropping out in the Guevgueli Complex (Saccani et al., 2008a), as well as continental arc sequences in the Paikon massif (Bébién et al., 1987; Brown and Robertson, 2004). To the west of the Paikon arc, several ophiolitic units have been recognized by Mercier (1966a). They are commonly known as Almopias ophiolitic units (Fig. 2b). While the External Ophiolites have been extensively studied in both Albanian and Greek sectors (e.g., Bortolotti et al., 2003; 2006; Dilek et al., 2008; Saccani et al., 2011; Robertson, 2012; Bortolotti et al., 2013, for exhaustive references), the Paikon Massif and the Almopias ophiolites are comparatively poorly known. Most of the works on these ophiolites date back to 1970-1990 decades and are rarely supported by adequate chemical and biostratigraphic data (e.g., Mercier, 1966a; 1966b; 1966c; Bébién and Cagny, 1979; Bébién, 1983; Vergély, 1984;

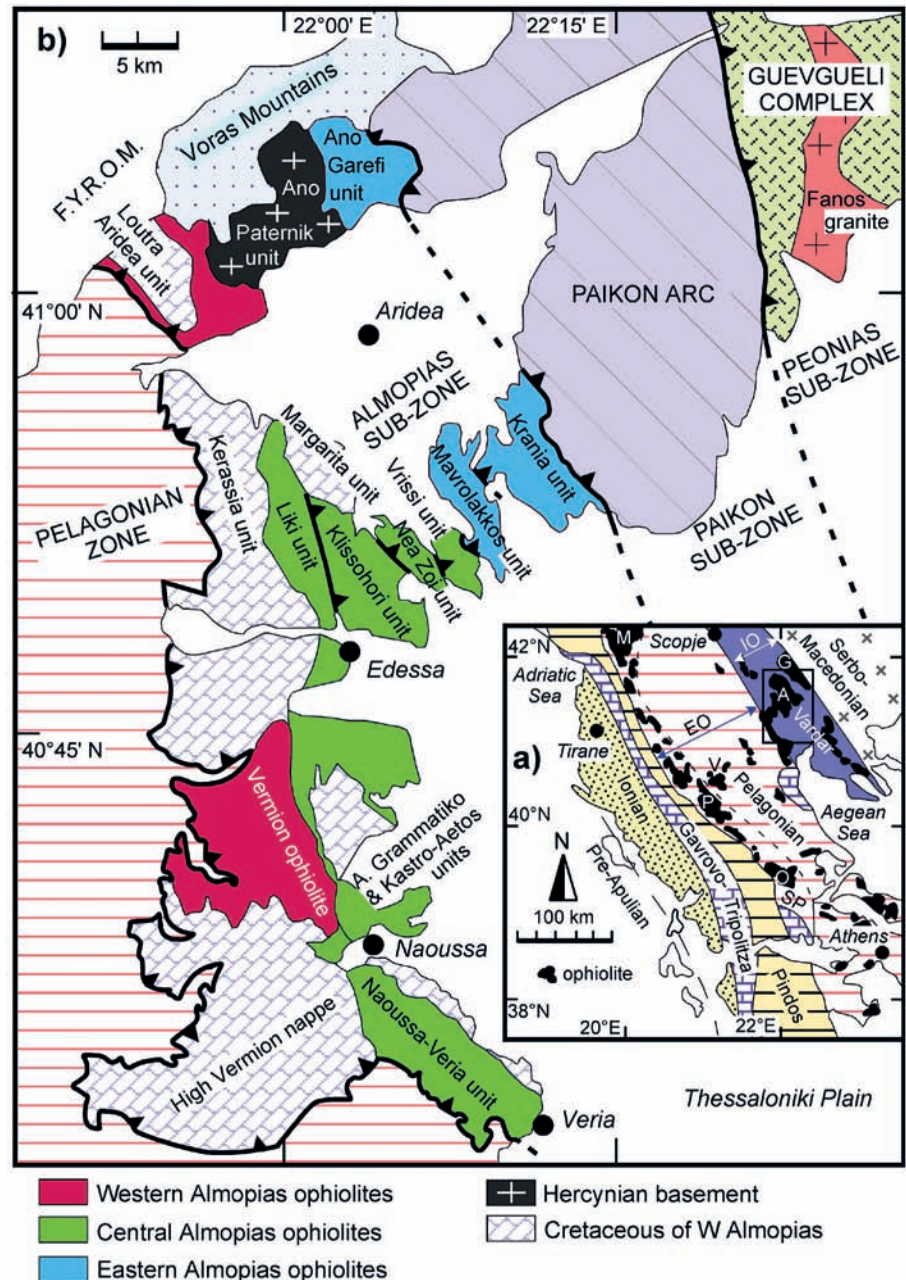


Fig. 2 - a) Tectono-stratigraphic zones of the Dinaric-Hellenic belt (modified from Saccani et al., 2011 and Robertson, 2012). The Pelagionian zone includes the Subpelagionian zone, according to Ferrière et al. (2012) and Borlototti et al. (2013). The box indicates the area expanded in panel b). Abbreviations in panel a): EO- External Ophiolites; IO- Internal Ophiolites; SP- Subpelagionian zone; M- Mirdita ophiolites, P- Pindos, V- Vourinos, O- Othrys, G- Guevgueli, A- Almopias. b) Geological sketch-map of the Vardar zone in the northern Greece (modified from Fig. 91 in Pe-Piper and Piper, 2002; Sharp and Robertson, 2006; Saccani et al., 2008b).

Bébién et al., 1987; 1994; Staïs et al., 1990). Moreover, in these works no biostratigraphic data on radiolarian cherts stratigraphically associated to volcanic rocks are presented. Relatively recent works have been carried out on the Paikon massif (Brown and Robertson, 2004), and Almopias ophiolites (De Wever, 1995; Sharp and Robertson, 1994; 2006; Saccani et al., 2008b). Only sparse geochemical and age data are available for these ophiolites (see Sharp and Robertson, 2006 for an exhaustive review). However, they were likely formed in the oceanic sector close to the Eurasian continental margin. The main purpose of this paper is thus to present preliminary geochemical and biostratigraphic data on the Almopias ophiolites and the associated arc-type Paikon unit, in order to decipher their original tectono-magmatic setting of formation. The presented biostratigraphic data are obtained from radiolarian cherts stratigraphically associated to volcanic rocks. Such approach made it possible to constrain in time the different magmatic and geodynamic events that are recorded in the studied units.

GEOLOGICAL SETTING

The vardarian ophiolitic bodies cropping out in the Vardar area include the Almopias and Peonias (also reported as Guevgueli) ophiolites, which are separated by the Paikon volcanic arc (Bébién et al., 1987; 1994; Staïs and Ferrière, 1991) (Fig. 2b). These different ophiolitic and volcanic arc units were formed in different oceanic and continental domains (Mercier, 1966c; Mercier et al., 1975; Bébién et al., 1994; Brown and Robertson, 2004; Saccani et al., 2008a; 2008b; 2011). Mercier (1966a) subdivided the Vardar zone in northern Greece into three sub-zones, which are (from east to west): the Peonias, Paikon, and Almopias (Fig. 2b). We are convinced that this type of subdivision should be abandoned because it may generate confusion between actual geographic location of ophiolites and their origin. In fact, Ferrière et al. (2012), used the terms Almopias, Paikon, and Peonias zones for stressing their distinct genetic significance. Nonetheless, a re-definition of the terminology of the different

units in the Vardar area needs further detailed research. Therefore, in this paper we will follow the Mercier (1966a) subdivision, because it is still widely used in literature.

The Peonias sub-zone

The Peonias sub-zone includes pre-Mesozoic basement, Triassic rift-related sedimentary rocks passing up into continental margin turbidites, Jurassic ophiolites, island arc volcanic rocks and granodioritic intrusions that are unconformably overlain by Late Jurassic sedimentary rocks (Pe-Piper and Piper, 2002, pp. 167-168). The Peonias sub-zone includes the Guevgueli ophiolitic complex, which consists of a Middle and Late Jurassic (Danelian et al., 1996; Kukoč et al., 2015) ophiolite sequence closely associated with calc-alkaline volcanics and dykes (Saccani et al., 2008a) and intruded by the granitoid intrusive complex of the Fanos granite (Bébién, 1983; Sarič et al., 2008). The Guevgueli ophiolites are considered to have formed in an ensialic back-arc basin opening to the north of the Paikon arc during Middle to Late Jurassic (Bébién, 1983; Bébién et al., 1987; Brown and Robertson, 2004; Saccani et al., 2008a).

The Paikon sub-zone

In the Paikon massif, the Hercynian basement is overlain by the Triassic to Early-Middle Jurassic Gandatch Formation, which consists of marbles, chloritic schists and calc-schists (Mercier, 1968; Brown and Robertson, 2003). According to these authors, the protoliths of these metamorphic rocks were probably represented by deposits belonging to a continental slope succession. The overlying (?) Jurassic Livadia Formation includes metavolcanic rocks mainly represented by rhyolites and minor meta-andesites and meta-basalts (Davis et al., 1988). This formation is conformably overlain by the (?) Middle Jurassic platform carbonates of the Gropi Formation. The overlying Late Jurassic Kastaneri formation includes intermediate to felsic tuffs, ignimbrites and rhyolites and minor interbedded algal limestone, sandstone and conglomerates (Davis et al., 1988; Mercier, 1968). The Kastaneri Formation is locally overlain unconformably by the Kimmeridgian - Tithonian Kromni limestones (Mercier, 1968; Brown and Robertson, 2003). The lower part of the Paikon sequence (Gandatch, Livadia, and Gropi formations) is affected by low-grade blueschist facies metamorphism. In contrast, the unconformably overlying formations are unaffected by high-pressure metamorphism (Sharp and Robertson, 2006).

Only sparse chemical analyses of volcanic rocks from the Paikon sub-zone are available in literature. Mafic rocks of the Gandatch and Livadia formations are principally basaltic andesites and andesites (Bébién et al., 1987; Davis et al., 1988). Bébién et al. (1994) suggested that volcanic rocks from the Livadia Formation are island arc tholeiites, boninites and minor felsic differentiates. Basalts and basaltic andesites of the Kromni Formation resemble island-arc tholeiites, though mid-ocean ridge and boninitic lavas are also present (Bébién et al., 1994).

The geochemistry of the magmatic rocks from Paikon unit indicate that they were originated in an arc setting developed during the Middle to Late Jurassic times in consequence of an east-dipping (present-day coordinates) oceanic subduction (Mercier, 1966c; Vergély and Mercier, 2000; Brown and Robertson, 2004). Brown and Robertson (2004) suggested that the Paikon represents a continental fragment bounded by oceanic basins in the Almopias and Peonias sub-zones.

The Almopias sub-zone

The Almopias sub-zone is tectonically very complex and it has been subdivided into several tectonic units by Mercier (1966a). Most of these units consist of Jurassic and subordinate Triassic ophiolites and related sedimentary covers (e.g., Staïs et al., 1990; Pe-Piper and Piper, 2002, pp. 154-158). The ophiolitic units can be grouped into the western, central, and eastern Almopias ophiolites (Fig. 2b).

According to Saccani et al. (2008b), the units from the western Almopias ophiolites in the Vermion Mountain consist of ophiolitic mélanges and harzburgitic mantle tectonites. Mélanges underwent greenschist to amphibolite metamorphic facies conditions associated with intense deformation. Magmatic protoliths within mélanges show various geochemical affinities, including both normal (N-) and enriched (E-) mid-ocean ridge basalt (MORB), alkaline ocean island basalt (OIB), low-Ti island arc tholeiite (IAT), very low-Ti boninitic, and calc-alkaline affinities. Ophiolites are unconformably covered by Late Jurassic-Early Cretaceous, shallow-water conglomerates and arenites. The Loutra Aridea unit (Fig. 2b) consists of an ophiolitic mélange, which is tectonically overlain by tectonic slices of serpentinitized harzburgite and chromite-bearing dunite. The ophiolites are locally unconformably overlain by conglomerates with ophiolitic clasts and transgressive Cretaceous limestones showing a Late Aptian to Middle Albian foraminiferal fauna (Mercier, 1966a).

The central Almopias ophiolites include the Liki, Klissohori, Nea Zoi, Vrissi, and Veria units (Fig. 2b). The Liki, Klissohori, and Nea Zoi units consist of strongly foliated ophiolitic mélanges (Mercier and Vergély, 1972; Sharp and Robertson, 1994). Large blocks mainly consist of serpentinites and marbles. The pervasive deformation postdates the Late Jurassic fossiliferous limestones in the mélange and predates the unconformably overlying Late Cretaceous limestones and was the result of dextral strike-slip deformation (Mercier and Vergély, 1972). Bijon (1982) described IATs and mafic boninites from the Liki and Klissohori units. However, Sharp and Robertson (2006) described some basaltic blocks showing OIB-type chemistry. In contrast, the Veria ophiolites in the southwest Almopias sub-zone (Fig. 2b) do not display metamorphic deformation and consist of ophiolite-bearing mélange units, which include tectonic slivers of mantle harzburgites and magmatic rocks showing N- and E-MORB, IAT, and boninitic affinities (Saccani et al., 2008b). The Vrissi unit consists of a mélange where slices of Triassic lavas, radiolarites and Late Cretaceous arenites are set in a foliated matrix (Staïs et al., 1990).

The eastern Almopias ophiolites (Fig. 2b) include the Ano Garefi, Krania, and Mavrolakkos units (Bechon, 1981; Sharp and Robertson, 1994). The Ano Garefi ophiolite consists of serpentinitized harzburgitic tectonites underlying a dyke-lava unit (Migiros and Galeos, 1987). No cumulate rocks have so far been recognised and ultramafics are intruded by diabase dykes. The dyke-lava unit consists of massive and pillowed basalts cut by dykes of MORB to OIB affinity. Locally, they are interbedded with thin levels of shales and limestones containing detrital chromite. This feature is also observed in the western Almopias ophiolites in the Vermion Mountain (Saccani et al., 2008b). The ophiolite complex is overlain by Late Cretaceous conglomerates and sandstones passing upward to limestones and turbidites.

According to Sharp and Robertson (1994), in the Mavrolakkos and Krania units, the ophiolite comprises MORB

pillow lavas with minor hyaloclastites and local radiolarites. In the Krania unit, radiolarites show Tithonian age. The lavas are overlain by the Black Schist Member, consisting of turbidites represented by sandstones, micaceous mudstones, and interbedded lavas. This member is in turn overlain by the Radiolarite Member that includes radiolarites of Middle-Late Jurassic age in the Mavrolakkos unit (Staïs et al., 1990; De Wever, 1995), cherty argillites, siliceous mudstones, thin sandstones (Staïs and Ferrière, 1991; Sharp and Robertson, 1994). The entire sequence is topped by Early Cretaceous turbidites (Sharp and Robertson, 1994), which are cut by basaltic andesite dykes (Bébién et al., 1980) and rare quartz diorite dykes dated at 124 Ma (Bechon, 1981). Bertrand et al. (1994) obtained whole rock K-Ar ages of 110-134 Ma from basalt or diabase. In the east, the entire ophiolite sequence is cut by sills and dykes of granophyre and granite that were compared with the Fanos granite of the Guevgueli ophiolite by Sharp and Robertson (1994). Sharp and Robertson (1994; 2006) interpreted the Mavrolakkos and Krania units as a single ophiolite sheet known as the Meglenitsa Ophiolite.

Ophiolites of the Almopias sub-zone have been interpreted as derived from a former oceanic basin (Almopias Ocean, Brown and Robertson, 2004; Vardar Ocean, Borolotti et al., 2013) that subducted eastwards underneath the Serbo-Macedonian Massif. During the Late Jurassic, ophiolites from this ocean were obducted westwards onto the Pelagonian zone (Mercier et al., 1975; Bébién et al., 1994; Sharp and Robertson, 1994; Brown and Robertson, 2004). Saccani et al. (2008b) concluded that the western and central Almopias ophiolites in the Vermion Mountain have formed in an intra-oceanic island arc setting, as suggested by the widespread occurrence of SSZ-type ophiolites, such as IAT, boninites and depleted mantle harzburgites.

SAMPLING AND METHODS

Twenty-three samples of radiolarian cherts and forty-one samples of volcanic and subvolcanic rocks were collected from the Paikon and Almopias sub-zones. In the Almopias sub-zone, samples were taken from the central and northern sectors. In particular, in the central sector, sam-

pling was focused on the various tectonic units recognized by Mercier (1966a). The sampled units and location of samples is shown in Table 1. In mélangé units, magmatic rocks were only taken from consistent, large volcanic series, whereas small isolated blocks or clasts were disregarded. Volcanic rocks in both volcanic units (Mavrolakkos and Krania units) and mélangé units (Vrissi unit) are frequently cross cut by dykes (e.g., Fig. 3a), which were also sampled. After preliminary petrographic and geochemical analyses, some of the acidic lava flows from the Mavrolakkos unit resulted strongly altered and silicized and were thus disregarded in this paper (see Table 1).

Radiolarian cherts were basically sampled when they were clearly stratigraphically associated with volcanic rocks (e.g., Fig. 3b). Unfortunately, radiolarian cherts associated through primary contacts with volcanic rocks were found only in three localities (Fig. 4, Table 1).

Volcanic and subvolcanic rock samples were analyzed for major and some trace elements by X-ray fluorescence (XRF) on pressed-powder pellets using an automated ARL Advant-X spectrometer with the matrix correction method proposed by Lachance and Trail (1966). Accuracy and detection limits were determined using international standards run as unknown. Accuracy was better than 2 relative % for major oxides and 5 relative % for trace element determinations, while the detection limits for trace elements were: Ce = 8 ppm; Ba, Cu, Sc, La = 5 ppm; Zn, Ga, Nd = 3 ppm; Ni, Co, Cr, V, Rb, Sr, Pb, Zr, Y = 2 ppm; Nb, Th = 1 ppm. Volatiles were determined as loss on ignition at 1000°C. Thirty representative samples were chosen for additional trace element analyses, including the rare earth elements (REE), using a Thermo Series X-I inductively coupled plasma-mass spectrometer (ICP-MS). The accuracy and detection limits were calculated using results for international standard rocks with certified values and the blind standards included in the sample set. Accuracy was in the range of 1-8 relative %, with the exception of Nb and Ta (12%), and U (9%). Detection limits were (in ppm): Sr, Y, Zr = 0.05; Rb, Nb = 0.02; Hf, Ta, Th, U = 0.002; La, Ce = 0.005; other REE = 0.002. All analyses were performed at the Department of Physics and Earth Sciences of the University of Ferrara. Results are presented in Table 2.

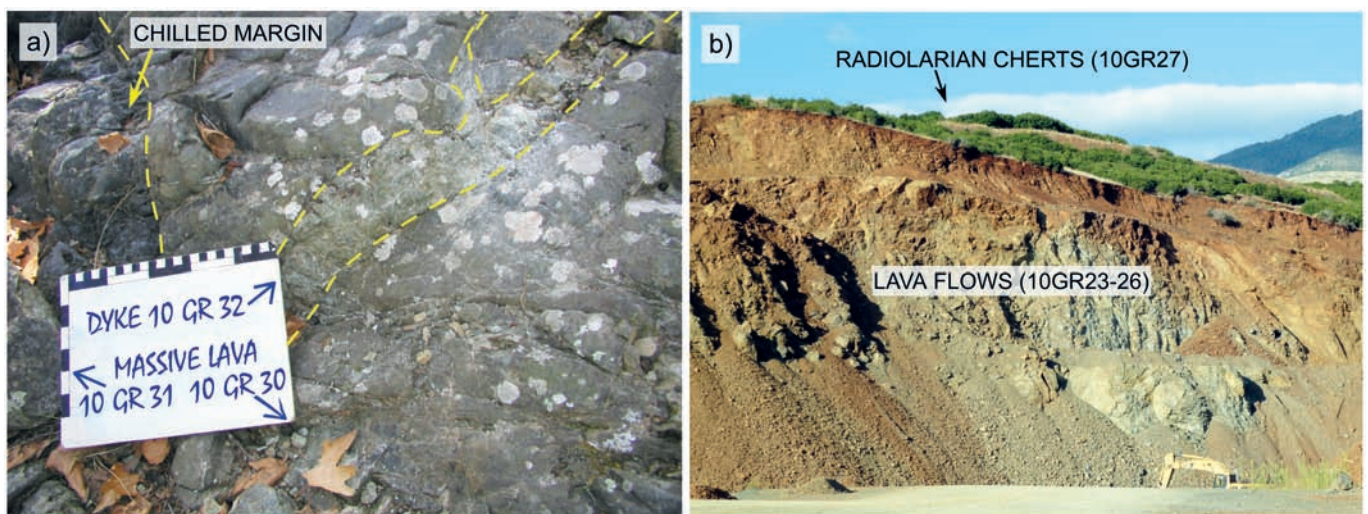


Fig. 3 - a) Close view of a low-K tholeiitic (subduction related) dyke intruding a volcanic sequence consisting of different lava flows showing normal mid-ocean ridge type (N-MORB) chemistry in the Vrissi unit. Lava flows show well-developed chilled margins. b) Field view of the massive lava flows topped by radiolarian cherts in the Krania unit.

Table 1 - Location and co-ordinates of the studied outcrops in the Paikon and Almopias sub-zones.

Stop	unit	Sample	Geografic co-ordinates	Note
1	Ano Garefi	10GR01	N 41 06 41.7, E 22 03 21.3	massive lava
		10GR02	N 41 06 41.7, E 22 03 21.3	microgabbro dyke in massive lava 10GR01
		10GR04	N 41 06 41.7, E 22 03 21.3	massive lava
		EP 82	N 41 05 36.96, E 22 02 51.15	mafic dyke in peridotites
2	Paikon	10GR05	N 41 04 02.7, E 22 05 28.7	massive meta-lava
3	Paikon	10GR06	N 41 04 8.5, E 22 05 34.3	tuffite
		EP 86	N 41 04 20.88, E 22 05 48.43	massive lava
		EP 87	N 41 04 20.82, E 22 05 57.07	massive lava
		EP 90	N 41 03 15.96, E 22 05 08.37	massive lava
		EP 91	N 41 03 16.07, E 22 04 58.66	massive lava
		EP 92	N 41 03 18.00, E 22 04 47.46	massive meta-lava
4	Mavrolakkos	10GR07	N 40 56 08.5, E 22 09 39.7	acidic volcanic rocks (disregarded)
5	Mavrolakkos	10GR08	N 40 54.889, E 22 09.813	dyke in 10GR09
		10GR09	N 40 54.889, E 22 09.813	massive lava
6	Mavrolakkos	10GR10	N 40 54 00.6, E 22 09 16.5	acidic volcanic rocks (disregarded)
		10GR11	N 40 54 00.6, E 22 09 16.5	acidic volcanic rocks (disregarded)
7	Mavrolakkos	10GR12	N 40 53.174, E 22 07.630	basalt dyke
8	Mavrolakkos	10GR13	N 40 53 21.1, E 22 08 06.2	pillow lava
		10GR14	N 40 53 21.1, E 22 08 06.2	dyke in pillow lava 10GR13
		10GR15	N 40 53 21.1, E 22 08 06.2	dyke in pillow lava 10GR13
		10GR16	N 40 53 21.1, E 22 08 06.2	dyke in pillow lava 10GR13
9	Mavrolakkos	10GR17	N 40 53 43.3, E 22 08 44.6	sheeted dyke complex
		10GR18	N 40 53 43.3, E 22 08 44.6	sheeted dyke complex
10	Krania	10GR19	N 40 53 27.6, E 22 10 39	dyke in massive lava 10GR20
		10GR20	N 40 53 27.6, E 22 10 39	massive lava
		10GR21	N 40 53 27.6, E 22 10 39	dyke in massive lava 10GR20
11	Krania	10GR22	N 40 53 29.5, E 22 11 02.4	pillow-lava
12	Krania	10GR23	N 40 53.074, E 22 12.854	massive lava
		10GR24	N 40 53.074, E 22 12.854	massive lava
		10GR25	N 40 53.074, E 22 12.854	massive lava
		10GR26	N 40 53.074, E 22 12.854	massive lava
		10GR27	N 40 53.074, E 22 12.854	red radiolarian cherts collected about 50 meters from 10GR26
13	Vrissi	10GR28	N 40 51.020, E 22 09.098	pillow lava
		10GR33	N 40 51.020, E 22 09.098	red radiolarian cherts at the top of pillow lava 10GR28
		10GR34	N 40 51.020, E 22 09.098	red siliceous siltstones at the top of pillow lavas
		10GR35	N 40 51.020, E 22 09.098	red radiolarian cherts along the road about 30 meters from pillow basalts
		10GR36	N 40 51.020, E 22 09.098	red siliceous siltstones along the road about 10 meters from pillow basalts
		10GR37	N 40 51.020, E 22 09.098	red siliceous siltstones about 1 meters from 10GR36
		10GR38	N 40 51.020, E 22 09.098	red radiolarian cherts near the basalt (uncertain stratigraphic position)
		10GR29	N 40 51 2.41, E 22 9 7.22	massive lava flow with bottom chilled margin
		10GR30	N 40 51 2.41, E 22 9 7.22	massive lava flow with bottom chilled margin
		10GR31	N 40 51 2.41, E 22 9 7.22	massive lava flow with bottom chilled margin
		10GR32	N 40 51 2.41, E 22 9 7.22	dyke in massive lava sequence 10GR29-31 (Fig. 2)

Table 1 (continues)

Stop	Unit	Sample	Geographic co-ordinates	Note
14	Nea Zoi	10GR39	N 40 49.856, E 22 08.340	red radiolarian cherts (base of the measured section)
		10GR39bis	N 40 49.856, E 22 08.340	red radiolarian cherts 10.50 meters from the base
		10GR40	N 40 49.856, E 22 08.340	red radiolarian cherts about 10 meters from the base
		10GR41	N 40 49.856, E 22 08.340	red radiolarian cherts 11.2 meters from the base
		10GR42	N 40 49.856, E 22 08.340	red radiolarian cherts 12.2 meters from the base
		10GR43	N 40 49.856, E 22 08.340	red radiolarian cherts 13.8 meters from the base
		10GR43bis	N 40 49.856, E 22 08.340	red radiolarian cherts about 25.0 meters from 10GR43
		10GR44	N 40 49.856, E 22 08.340	red radiolarian cherts about 5.0 meters from 10GR43bis
		10GR45	N 40 49.856, E 22 08.340	red radiolarian cherts about 10.0 meters from 10GR43bis
		10GR46	N 40 49.856, E 22 08.340	red radiolarian cherts about 35 meters from 10GR45
		10GR47	N 40 49.856, E 22 08.340	red radiolarian cherts 0.2 meters from 10GR46
		10GR48	N 40 49.856, E 22 08.340	red radiolarian cherts about 25 meters from 10GR46
		10GR49	N 40 49.856, E 22 08.340	red radiolarian cherts about 0.35 meters from the 10GR48
		15	Nea Zoi	10GR50
10GR51	N 40 50.073, E 22 08.413			massive lava
16	Nea Zoi	10GR52	N 40 50.009, E 22 08.485	massive lava
		10GR53	N 40 50.009, E 22 08.485	red radiolarian cherts about 5 metres from the basalts
		10GR54	N 40 50.009, E 22 08.485	red radiolarian cherts about 6.2 metres from the basalts
		10GR55	N 40 50.009, E 22 08.485	red radiolarian cherts about 6.9 metres from the basalts
17	Liki	EP78	N 40 51 40.68, E 22 01 58.54	amphibolite
		EP79	N 40 51 52.12, E 22 01 48.71	amphibolite

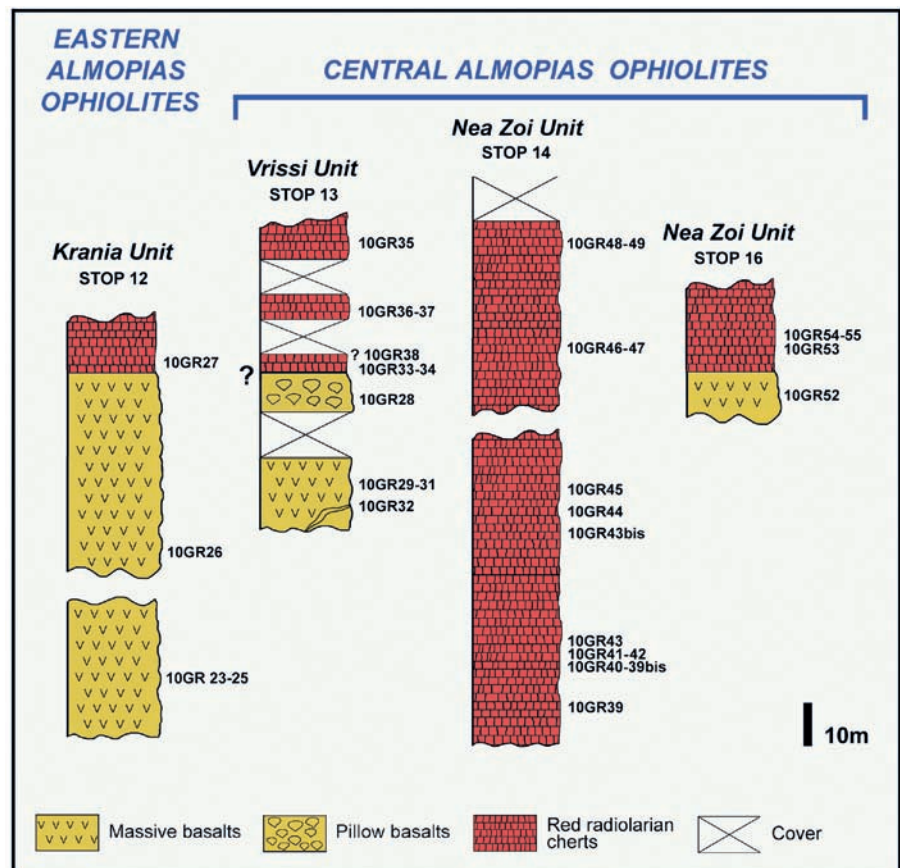


Fig. 4 - Schematic logs showing the mutual positions of the sampled volcanic rocks and radiolarian cherts in the Stops 12, 13, and 16 (AlmoPIas ophiolitic units). The thickness of the radiolarian cherts in the Nea Zoi Unit (Stop 14) is probably due to tectonic doubling.

Table 2 - Bulk-rock major and trace element analyses of selected samples from the Paikon and Almopias sub-zones.

Unit	Paikon unit							Ano Garefi unit			
	3	3	3	2	3	3	3	1	1	1	1
Stop											
Ass. Rad.											
Age											
Sample	EP92	EP86	EP87	10GR05	10GR06	EP90	EP91	10GR01	10GR02	10GR04	EP82
Rock	meta-bas	bas	bas	meta-dac	dac	rhy	and	bas	microgabbro	bas	bas
Group	3	4	4	5	5	5	5	1	1	1	2
Type	N-MORB	bon	bon	CAB	CAB	CAB	CAB	alk	alk	alk	E-MORB
Note	MLF	MLF	MLF	MLF	tuff	MLF	MLF	MLF	dyke in GR01	MLF	dyke in peridotite
<i>XRF analysis:</i>											
SiO ₂	44.20	48.87	48.63	69.87	66.62	73.40	58.12	48.84	44.57	48.78	44.37
TiO ₂	1.49	0.40	0.47	0.23	0.33	0.44	0.82	2.01	2.14	2.15	1.53
Al ₂ O ₃	12.57	15.60	15.73	13.62	14.60	13.05	19.78	15.12	15.77	15.56	18.34
Fe ₂ O ₃	1.69	1.95	1.87	0.62	0.76	0.41	0.62	1.26	1.38	1.30	1.24
FeO	11.27	12.99	12.47	4.16	5.08	2.72	4.12	8.43	9.19	8.69	8.24
MnO	0.42	0.30	0.25	0.05	0.07	0.04	0.08	0.14	0.17	0.14	0.18
MgO	9.23	11.95	12.32	6.90	5.99	3.26	6.04	10.19	11.68	10.21	9.06
CaO	9.66	1.11	1.21	0.16	0.32	0.16	0.25	5.91	7.26	4.14	10.78
Na ₂ O	1.38	1.33	1.21	0.06	2.70	4.03	7.14	4.24	2.95	3.60	1.05
K ₂ O	0.02	0.01	0.05	1.29	0.56	0.59	0.13	0.09	0.69	1.52	0.52
P ₂ O ₅	0.12	0.06	0.04	0.02	0.04	0.02	0.07	0.60	0.57	0.45	0.28
L.O.I.	8.02	5.03	5.35	3.11	3.03	1.92	2.86	3.19	3.71	3.46	4.48
Total	100.07	100.07	100.05	100.09	100.11	100.05	100.02	100.02	100.08	100.02	100.06
CO ₂	n.a.	n.a.	n.a.	n.a.	n.a.	n.a.	n.a.	n.a.	n.a.	n.a.	n.a.
Mg#	59.4	62.1	63.8	74.7	67.8	68.1	72.3	68.3	69.4	67.7	66.2
Zn	86	287	173	50	42	19	36	72	59	67	28
Cu	50	38	n.d.	n.d.	n.d.	13	n.d.	154	14	123	43
Sc	42	48	56	17	21	20	35	19	17	20	31
Ga	15	13	13	6	10	8	8	18	17	17	3
Ni	75	5	5	n.d.	n.d.	2	44	87	128	72	117
Co	40	36	36	8	13	3	15	42	45	41	33
Cr	269	21	18	n.d.	10	8	171	252	243	167	256
V	306	384	375	37	77	23	114	225	181	217	174
Ba	31	11	14	120	102	64	42	100	155	199	12
Pb	17	4	5	4	3	4	2	5	5	7	8
<i>ICP-MS and XRF (*) analysis:</i>											
Rb	0.853	0.217	0.712	10.6	3.61	8*	1.93	1.70	9.38	36.7	0.298
Sr	76.5	19.4	32.6	16.2	24.9	19*	61.5	852	1108	179	39.5
Y	29.3	7.54	7.73	27.5	29.3	30*	16.9	21.0	34.9	38.8	19.6
Zr	77.7	17.4	18.4	54.0	85.1	75*	95.4	176	184	194	92.8
La	3.04	0.384	0.531	18.7	16.0	n.d.*	14.0	22.6	29.3	31.0	7.92
Ce	9.75	1.14	1.66	35.8	33.8	8*	22.8	44.8	57.1	62.1	18.5
Pr	1.78	0.219	0.317	4.30	3.89		3.01	4.98	7.26	7.95	2.49
Nd	9.81	1.34	1.89	18.1	17.0	7*	11.3	18.2	29.5	32.8	10.9
Sm	3.30	0.521	0.716	4.52	4.32		3.19	4.22	6.66	7.53	2.83
Eu	1.20	0.250	0.337	0.783	0.649		0.513	1.28	2.03	2.34	1.16
Gd	4.51	0.882	1.13	3.92	3.60		3.49	3.76	6.66	7.70	3.05
Tb	0.813	0.175	0.224	0.575	0.525		0.552	0.631	1.04	1.23	0.536
Dy	5.49	1.30	1.58	3.50	3.18		3.32	3.68	5.88	7.07	3.28
Ho	1.20	0.304	0.374	0.695	0.656		0.639	0.738	1.18	1.43	0.700
Er	3.47	0.937	1.14	1.98	1.77		1.79	1.99	3.07	3.77	1.94
Tm	0.544	0.149	0.178	0.293	0.262		0.266	0.280	0.426	0.536	0.283
Yb	3.54	0.996	1.16	1.92	1.72		1.80	1.69	2.63	3.31	1.82
Lu	0.516	0.152	0.175	0.277	0.254		0.275	0.240	0.371	0.465	0.270
Nb	2.36	0.239	0.335	1.12	0.970	1*	1.50	36.9	44.9	46.8	9.69
Hf	2.43	0.457	0.550	0.458	0.432		1.24	4.30	4.55	4.25	2.42
Ta	0.154	0.021	0.027	0.088	0.067		0.097	0.223	2.15	2.33	0.479
Th	0.129	0.100	0.105	1.57	1.46	2*	1.48	1.91	2.10	2.83	0.519
U	0.056	0.043	0.060	0.192	0.178		0.140	0.737	0.712	0.835	0.148
Ti/V	32	7	8					55	73	62	55
Nb/Y	0.08	0.03	0.04	0.04	0.03	0.04	0.09	1.68	1.40	1.34	0.49
(La/Sm) _N	0.60	0.48	0.48	2.67	2.40		2.84	3.46	2.83	2.66	1.81
(Sm/Yb) _N	1.03	0.58	0.68	2.62	2.78		1.97	2.78	2.82	2.53	1.73
(La/Yb) _N	0.62	0.28	0.33	6.98	6.67		5.61	9.61	7.98	6.72	3.12

Table 2 (continues)

Unit	Krania unit								Mavrolakkos unit					
Stop	12	12	12	12	10	10	10	11	5	5	7	8	8	8
Ass. Rad.				10GR27										
Age				M-L Jr.										
Sample	10GR23	10GR24	10GR25	10GR26	10GR19	10GR20	10GR21	10GR22	10GR08	10GR09	10GR12	10GR13	10GR14	10GR15
Rock	Fe-bas	Fe-bas	bas	Fe-bas	bas	rhy	bas and	and	bas	bas	bas	bas	Fe-bas	Fe-bas
Group	3	3	3	3	6	5	5	5	3	3	3	3	3	3
Type	N-MORB	N-MORB	N-MORB	N-MORB	LK-T	CAB	CAB	CAB	N-MORB	N-MORB	N-MORB	N-MORB	N-MORB	N-MORB
Note	MLF	MLF	MLF	MLF	dyke in GR20	MLF	dyke in GR20	pillow	dyke in GR09	MLF	dyke	pillow	dyke in GR13	dyke in GR13
<i>XRF analysis:</i>														
SiO ₂	48.53	47.10	50.05	48.09	47.42	71.60	55.00	57.14	48.22	46.91	51.08	50.85	49.54	48.42
TiO ₂	2.22	2.31	0.80	2.26	0.60	0.39	0.84	0.75	1.86	1.85	1.42	1.15	1.92	2.60
Al ₂ O ₃	13.26	13.21	16.32	13.86	16.02	14.83	14.91	18.00	14.78	14.28	13.40	15.37	13.66	14.15
Fe ₂ O ₃	1.94	2.10	1.07	1.88	1.47	0.34	0.57	1.03	1.71	1.42	1.47	1.20	1.77	2.30
FeO	12.93	14.03	7.11	12.51	9.82	2.27	3.83	6.85	11.40	9.46	9.80	8.02	11.82	15.33
MnO	0.22	0.23	0.15	0.20	0.20	0.08	0.19	0.04	0.14	0.13	0.19	0.17	0.19	0.22
MgO	5.91	6.78	8.22	5.62	9.40	0.98	6.04	3.06	6.77	4.53	7.43	7.78	5.58	3.92
CaO	9.38	8.61	8.62	9.20	5.56	0.83	8.57	2.90	6.60	10.22	10.11	7.55	10.31	6.82
Na ₂ O	3.24	3.07	2.70	3.68	1.27	7.08	4.85	0.24	3.16	3.75	2.24	3.97	2.95	3.68
K ₂ O	0.35	0.39	1.89	0.12	2.62	0.60	0.31	3.75	0.58	0.59	0.72	0.86	0.05	0.04
P ₂ O ₅	0.20	0.16	0.07	0.21	0.06	0.11	0.23	0.09	0.17	0.20	0.15	0.15	0.18	0.43
L.O.I.	1.89	1.97	3.01	2.44	5.61	1.05	4.71	6.17	4.70	6.75	2.05	2.96	2.08	2.13
Total	100.05	99.96	100.02	100.07	100.05	100.17	100.05	100.02	100.10	100.08	100.06	100.03	100.04	100.04
CO ₂	n.a.	n.a.	n.a.	n.a.	n.d.	n.a.	n.d.	n.d.	n.d.	1.30	n.a.	n.a.	n.a.	n.a.
Mg#	44.9	46.3	67.3	44.4	63.0	43.4	73.8	44.4	51.4	46.04	57.4	63.3	45.7	31.3
Zn	92	95	54	103	58	41	71	99	110	98	35	50	76	145
Cu	56	56	70	55	22	n.d.	10	61	15	51	26	37	53	19
Sc	45	46	28	48	34	8	24	12	52	48	41	30	40	41
Ga	16	17	13	16	14	12	14	21	18	18	15	10	15	22
Ni	42	35	90	40	23	n.d.	7	69	40	43	45	47	38	12
Co	51	51	44	51	42	4	13	16	53	55	42	43	47	44
Cr	142	194	362	150	129	2	31	90	154	151	227	258	56	37
V	435	453	250	466	378	7	302	125	388	361	331	289	405	429
Ba	69	62	39	87	202	123	74	392	96	88	77	490	59	85
Pb	6	6	5	7	6	2	6	24	8	7	4	4	7	5
<i>ICP-MS and XRF (*) analysis:</i>														
Rb	7.94	5*	25.6	1.86	41.9	11*	3.61	48.9	17*	17.6	6*	11.4	0.684	n.d.*
Sr	95.6	69*	64.7	121	246	71*	289	43.3	163*	159	156*	227	110	111*
Y	46.9	50*	26.0	21.7	13.8	34*	32.8	17.0	39*	33.6	26*	23.7	42.6	69*
Zr	132	159*	58.5	127	27.1	116*	84.9	216	136*	108	79*	68.8	108	234*
La	5.75	7*	2.94	1.83	4.31	9*	14.8	9.99	n.d.*	4.69	n.d.*	2.63	5.12	10*
Ce	17.5	18*	8.09	5.87	10.5	25*	31.3	20.0	n.d.*	12.9	8*	7.74	13.9	27*
Pr	2.92		1.36	1.00	1.39		4.29	2.33		2.09		1.29	2.24	
Nd	15.0	12*	6.64	5.60	6.57	15*	18.5	9.89	11*	10.9	9*	6.82	11.5	24*
Sm	4.83		2.19	2.02	1.96		4.61	2.76		3.62		2.25	3.99	
Eu	1.57		0.667	0.658	0.697		1.23	0.905		1.22		0.868	1.30	
Gd	5.75		2.96	2.97	2.24		4.71	2.64		4.43		3.16	4.93	
Tb	1.07		0.553	0.581	0.387		0.789	0.399		0.796		0.563	0.964	
Dy	7.15		3.74	4.13	2.53		4.85	2.38		5.41		3.83	6.36	
Ho	1.56		0.840	0.940	0.553		1.05	0.464		1.17		0.833	1.42	
Er	4.29		2.35	2.66	1.54		2.93	1.27		3.23		2.33	3.97	
Tm	0.638		0.373	0.416	0.231		0.425	0.189		0.489		0.353	0.597	
Yb	4.15		2.37	2.72	1.43		2.70	1.22		3.14		2.31	3.89	
Lu	0.626		0.357	0.397	0.199		0.393	0.187		0.459		0.339	0.594	
Nb	6.42	5*	2.30	5.22	2.88	2*	3.68	4.92	4*	5.01	2*	2.30	3.83	6*
Hf	3.64		1.58	3.12	1.94		0.695	2.33		2.68		1.83	3.30	
Ta	0.380		0.172	0.285	0.178		0.218	0.436		0.278		0.151	0.254	
Th	0.218	1*	0.325	0.190	0.972	4*	2.13	6.36	n.d.*	0.282	n.d.*	0.111	0.379	n.d.*
U	0.047		0.106	0.066	0.417		0.403	2.56		0.122		0.062	0.124	
Ti/V	31	31	20	30	10		18		30	33	26	25	29	37
Nb/Y	0.14	0.10	0.10	0.23	0.24	0.07	0.12	0.31	0.11	0.14	0.09	0.09	0.10	0.09
(La/Sm) _N	0.77		0.87	0.59	1.42		2.06	2.34		0.84		0.76	0.83	
(Sm/Yb) _N	1.29		1.03	0.82	1.52		1.90	2.50		1.28		1.08	1.14	
(La/Yb) _N	0.99		0.89	0.48	2.16		3.92	5.85		1.07		0.82	0.94	

Abbreviations: bas- basalt; bas and- basaltic andesite; Fe-bas- ferrobassalt; and- andesite; dac- dacite; rhy- rhyolite; amph.te- amphibolite; MORB- mid-ocean ridge basalts; N- normal-type; E- enriched-type; alk- alkaline; bon- boninite; CAB- calc-alkaline; LKT- low K tholeiites; MLF- massive lava flow; sh-dy- sheeted dyke; n.a.- not analyzed; n.d.- not detected. Fe₂O₃ = 0.15 x FeO; Mg# = molar Mg/(Mg+Fe)*100. Radiolarian cherts samples stratigraphically associated with volcanic rocks (Ass. Rad.) and their ages are also shown. Abbreviations, M- Middle; L- Late; Tr- Triassic; Jr- Jurassic.

Table 2 (continues)

Unit	Mavrolakkos unit			Vrissi unit					Nea Zoi unit			Liki unit	
Stop	9	9	8	13	13	13	13	13	15	15	16	17	17
Ass. Rad.							GR33-37				GR53-55		
Age							M-L Jr				L Tr		
Sample	10GR17	10GR18	10GR16	10GR29	10GR30	10GR31	10GR28	10GR32	10GR50	10GR51	10GR52	EP78	EP79
Rock	bas	bas	and	bas	Fe-bas	Fe-bas	bas	bas	bas	rhy	bas	amph.te	amph.te
Group	3	3	6	3	3	3	6	6	3	5	5	3	6
Type	N-MORB	N-MORB	LK-T	N-MORB	N-MORB	N-MORB	LK-T	LK-T	N-MORB	CAB	CAB	N-MORB	LK-T
Note	sh-dy	sh-dy	dyke in GR13	MLF	MLF	MLF	pillow	dyke in GR29-31	MLF	MLF	MLF		
<i>XRF analysis:</i>													
SiO ₂	49.69	50.45	57.85	50.22	48.06	48.35	41.36	47.37	48.73	69.54	49.30	49.96	57.07
TiO ₂	1.17	1.24	0.81	1.28	2.25	2.58	0.77	0.70	0.91	0.70	0.84	1.81	0.97
Al ₂ O ₃	17.42	16.79	9.83	14.97	13.87	14.20	11.67	14.12	16.26	12.75	16.88	12.94	15.03
Fe ₂ O ₃	1.31	1.31	1.08	1.29	1.83	2.30	0.87	0.73	1.03	0.75	0.79	1.84	0.98
FeO	8.70	8.73	7.17	8.61	12.19	15.35	5.82	4.87	6.89	4.97	5.27	12.28	6.55
MnO	0.18	0.18	0.13	0.16	0.19	0.20	0.18	0.08	0.15	0.10	0.12	0.23	0.15
MgO	6.77	6.44	5.95	7.84	6.92	3.78	7.26	2.84	8.41	3.15	6.72	6.87	5.01
CaO	7.56	7.73	13.46	8.17	7.21	6.29	17.48	23.00	11.16	1.35	11.94	9.04	6.78
Na ₂ O	3.09	3.48	0.46	3.46	4.23	3.76	3.60	n.d.	2.44	1.85	2.91	1.76	4.31
K ₂ O	1.70	1.37	0.11	0.83	0.12	0.04	0.07	0.03	0.59	1.46	1.29	1.69	1.81
P ₂ O ₅	0.11	0.11	0.09	0.15	0.26	0.43	0.08	0.07	0.09	0.13	0.05	0.17	0.10
L.O.I.	2.35	2.17	3.06	2.98	2.89	2.79	10.92	6.26	3.37	3.26	4.00	1.42	1.27
Total	100.05	100.00	100.00	99.96	100.01	100.07	100.09	100.06	100.01	100.00	100.09	100.01	100.03
CO ₂	n.a.	n.a.	0.91	n.a.	n.a.	n.a.	7.09	1.89	n.a.	n.a.	n.a.	n.a.	n.a.
Mg#	58.1	56.8	59.66	61.9	50.3	30.5	68.95	50.98	68.5	53.1	69.4	49.9	57.7
Zn	79	65	43	61	115	144	48	3	51	59	50	105	53
Cu	53	56	37	68	45	14	22	23	85	17	20	63	5
Sc	30	35	31	38	40	38	24	22	40	10	34	48	29
Ga	14	14	17	9	16	24	12	30	12	10	12	16	14
Ni	46	44	206	52	23	7	115	33	66	80	149	66	58
Co	43	44	44	46	53	49	38	18	42	20	81	43	33
Cr	141	155	359	233	154	33	450	77	429	188	464	198	215
V	317	345	192	286	412	444	214	195	231	78	222	411	186
Ba	104	96	5	276	69	68	34	34	128	285	49	182	379
Pb	2	4	6	5	5	6	8	2	5	18	4	9	4
<i>ICP-MS and XRF (*) analysis:</i>													
Rb	19.5	18*	0.593	11.6	1.58	n.d.*	0.780	0.884	10.6	53.0	18*	32.4	39.9
Sr	164	147*	22.9	161	62.2	75*	190	34.2	192	76.2	163*	64.0	79.0
Y	14.7	22*	22.1	31.7	69.0	68*	17.0	21.2	17.3	10.5	16*	44.9	14.6
Zr	51.7	55*	62.9	88.3	199	238*	57.4	39.6	48.3	162	47*	111	71.7
La	1.38	n.d.*	4.04	3.18	8.37	8*	4.68	2.30	1.62	10.8	n.d.*	3.32	5.09
Ce	4.37	n.d.*	9.49	9.69	23.7	26*	11.2	6.36	5.05	23.6	8*	11.6	11.9
Pr	0.741		1.49	1.75	3.91		1.55	1.03	0.99	3.19		2.06	1.61
Nd	3.90	5*	7.17	8.98	21.0	22*	7.46	5.43	5.21	13.1	4*	11.5	7.03
Sm	1.30		2.31	2.96	6.81		2.43	1.94	1.79	3.08		4.05	2.16
Eu	0.542		0.784	0.858	1.91		0.873	0.887	0.681	0.550		1.44	0.68
Gd	1.87		2.66	3.97	8.29		2.86	2.50	2.39	2.92		5.61	2.65
Tb	0.347		0.479	0.724	1.56		0.501	0.482	0.425	0.389		1.05	0.459
Dy	2.44		3.23	4.81	10.54		3.30	3.15	2.77	2.10		7.05	2.85
Ho	0.544		0.733	1.05	2.31		0.715	0.712	0.601	0.413		1.58	0.613
Er	1.58		2.10	2.89	6.37		2.06	2.01	1.76	1.12		4.46	1.67
Tm	0.243		0.321	0.430	0.935		0.305	0.307	0.266	0.160		0.675	0.250
Yb	1.61		2.15	2.79	5.96		1.97	1.97	1.70	1.03		4.42	1.65
Lu	0.242		0.342	0.408	0.872		0.291	0.301	0.253	0.146		0.658	0.252
Nb	1.60	2*	0.734	2.81	6.54	6*	1.29	1.52	1.60	6.14	1*	2.46	3.49
Hf	1.40		2.23	2.46	5.40		1.33	1.20	1.24	0.60		1.27	1.64
Ta	0.113		0.065	0.224	0.375		0.092	0.129	0.106	0.369		0.175	0.291
Th	0.098	n.d.*	0.493	0.187	0.487	n.d.*	0.627	0.291	0.071	4.13	3*	0.134	1.03
U	0.045		0.189	0.068	0.154		0.161	0.120	0.032	1.31		0.070	0.611
Ti/V	23	22		28	34	36	27	23	24		24	27	
Nb/Y	0.11	0.07	0.04	0.09	0.11	0.09	0.09	0.08	0.08	0.51	0.06	0.06	0.22
(La/Sm) _N	0.68		1.13	0.69	0.79		1.24	0.77	0.58	2.26		0.53	1.52
(Sm/Yb) _N	0.90		1.19	1.18	1.27		1.37	1.10	1.17	3.32		1.02	1.45
(La/Yb) _N	0.61		1.34	0.82	1.01		1.70	0.84	0.68	7.52		0.54	2.21

Twenty-three samples of radiolarian cherts (Fig. 4, Table 1) were etched with hydrochloric and hydrofluoric acid at different concentrations.

RADIOLARIAN AGES

The Late Triassic samples yielded radiolarians with very poor preservation (Plate 1.1-1.6) while in the Middle-Late Jurassic samples the preservation of radiolarians varies between poor and moderate (Plate 1.7-1.21). For taxonomy and ranges of the Late Triassic radiolarian markers we referred mainly to De Wever et al. (1979), Tekin (1999), Hauser et al. (2001), Bragin (2007), Chiari et al. (2012), while for the taxonomy and ranges of the Middle-Late Jurassic markers we referred to Baumgartner et al. (1995a), Dumitrica et al. (1997), Hull (1997), Chiari et al. (1997; 2004a; 2004b; 2008), Danelian et al. (2006), O'Dogherty et al. (2006), Nirta et al. (2010), Goričan et al. (2012), Jach et al. (2014), Krische et al. (2014), Kukoč et al. (2015). We adopted the radiolarian zonation based on Unitary Association Zones (UAZ) proposed by Baumgartner et al. (1995b). Moreover for radiolarian genera we followed the taxonomy proposed by O'Dogherty et al. (2009a; 2009b).

Krania Unit

Stop n. 12 (Figs. 3b, 4)

10GR27: This sample contains few radiolarians in moderate preservation; the presence of *Archaeodictyomitra patricki* Kocher (Plate 1.7) could indicate a late Bajocian to late Kimmeridgian-early Tithonian age (UAZ 4-11, Middle-Late Jurassic). The range of this taxon could be tentatively assigned to UAZ 4-11 due to its presence in samples of: 1) middle Callovian-early Oxfordian to middle-late Oxfordian age (UAZ 8-9, sample TERR in Chiari et al., 1997); 2) middle Bathonian to late Bathonian-early Callovian age (UAZ 6-7, samples VS3 and VS4 in O'Dogherty et al., 2006); 3) middle Callovian-early Oxfordian to late Oxfordian-early Kimmeridgian age (UAZ 8-10, sample PK35 in Jach et al., 2014); 4) late Bajocian to latest Bajocian-early Bathonian (UAZ 4-5, sample GRA14 in Nirta et al., 2010); 5) latest Bajocian-early Bathonian to late Bathonian-early Callovian age? (UAZ 5-7?, sample L89, Krische et al., 2014); 6) middle Callovian-early Oxfordian to late Kimmeridgian-early Tithonian age (UAZ 8-11, samples Mg-2 and Mg-29 in Danelian et al., 2006); 7) late Bathonian-early Callovian age (UAZ 7, sample RADS 4, Kukoč et al., 2015).

Vrissi Unit

Stop n. 13 (Fig. 4)

10GR34: The sample contains abundant radiolarians in poor and moderate preservations (Plate 1.8-1.21). The presence of *Emiluvia pessagnoii multipora* Steiger with *Cingoloturris carpatica* Dumitrica, *Emiluvia pentaporata* Steiger and Steiger, *Eucyrtidiellum ptyctum* (Riedel and Sanfilippo) (range respectively: UAZ 8-14, UAZ 7-11, UAZ 11-11 and UAZ 5-11 in Baumgartner et al. 1995b) indicate a late Kimmeridgian-early Tithonian age (UAZ 11, Late Jurassic). It is worth of note that it is possible to indicate a broader range (UAZ 8-11) for *Emiluvia pentaporata* Steiger and Steiger (= *Emiluvia bisellea* Danelian in Baumgartner et al. 1995a, range UAZ 11-11) as reported in Chiari et al. (2004a), Danelian et al. (2006) and Chiari et al.

(2008). Therefore the age of the sample 10GR34 is middle Callovian-early Oxfordian to late Kimmeridgian-early Tithonian age (UAZ 8-11, Middle-Late Jurassic). Furthermore the samples 10GR35, 10GR37 and 10GR38 collected in this section, contain radiolarians with very poor preservation and it is not possible indicate their ages. The samples 10GR33, 10GR36 are barren.

Nea Zoi Unit

Stop n. 14 (Fig. 4)

10GR40: This sample contains few radiolarians in very poor preservation, the presence of genus *Nakasekoellus* (*Nakasekoellus* sp., Plate 1.2; range in O'Dogherty et al., 2009a) indicate a late Carnian-middle Norian age (Late Triassic). In this paper we consider *Nakasekoellus* Kozur as senior synonym of *Xipha* Blome as reported in Tekin (1999).

10GR42: Due to the presence of *Capnuchosphaera constricta* (Kozur and Mock) (Plate 1.3; range in Tekin, 1999; Bragin, 2007) it is possible indicate a late Carnian-early Norian age (Late Triassic) for this sample. The other samples of this section (see Fig. 4) contain radiolarians with very poor preservation and it is not possible indicate exact ages.

Stop n. 16 (Fig. 4)

10GR53: The sample contain few radiolarians in very poor preservation and the presence of genus *Capnuchosphaera* (*Capnuchosphaera* sp., Plate 1.5; range in O'Dogherty et al., 2009a) indicate an early Carnian-middle Norian age. The other samples of this section, 10GR54 and 10GR55, contain radiolarians with very poor preservation.

PETROGRAPHY

Magmatic rocks from the Paikon and Almopias sub-zones were formed in a number of different eruptive (i.e., massive and pillowed lava flows, tuffs) and sub-volcanic (i.e., individual diabase and microgabbro dykes, sheeted dykes) styles. Moreover, these rocks show a wide range of magmatic fractionation spanning from basalt to basaltic andesite, andesite, dacite and rhyolite. Finally, magmatic rocks in the Liki unit underwent amphibolite metamorphic facies conditions associated with intense deformation, whereas in the other units, they record low-grade ocean floor metamorphism under static conditions. This results in a very complex scenario of petrographic types associated with the different geochemical groups. For this reason, the following petrographic description will be made with reference to the different geochemical groups that are presented in the next section.

Group 1 basalts show aphyric, sub-ophitic texture. The primary mineral phases consist of small laths of plagioclase and interstitial clinopyroxene. Group 1 and Group 2 dykes show coarse-grained, ophitic texture with euhedral plagioclase enclosed into subhedral clinopyroxene. All these rocks underwent severe alteration. Plagioclase is completely altered in clay minerals and, occasionally, epidote and saussurite, whereas clinopyroxene is commonly transformed into chlorite.

Group 3 rocks show a variety of textures. Sample EP92 from the Paikon unit displays a weak foliation and the primary minerals are completely transformed into chlorite, albite and epidote. Sheeted dykes and massive lavas from the

Krania and Mavrolakkos units have porphyritic and glomeroporphyritic texture with microphenocrysts of plagioclase and locally olivine and clinopyroxene. The porphyritic index (PI) varies from 10 to 30. In massive lava samples from the Krania unit, groundmass textures include cryptocrystalline and intersertal varieties, whereas in samples from the Mavrolakkos unit groundmass shows intergranular texture. Pillow lavas, massive lavas and individual dykes show subophytic to intersertal textures with euhedral laths of plagioclase and subhedral clinopyroxene. Locally, both skeletal and subhedral opaque minerals are abundant. Only sample 10GR30 (massive lava flow) from the Vrissi unit shows porphyritic texture (PI = 25), where phenocrysts consist of plagioclase and minor clinopyroxene. Groundmass in these rocks varies from microcrystalline to medium-grained. All Group 3 rocks show high degrees of alteration, which mainly resulted in the crystallization of secondary chlorite and clay minerals.

Group 4 basalts show microcrystalline foliated texture, where only small laths of altered plagioclase can be recognized. The foliated texture is marked by layers of very fine-grained chlorite.

Group 5 and Group 6 rocks display different types of textures. Sample 10GR05 from the Paikon unit shows very fine-grained, foliated texture, where epidote, chlorite and quartz can be recognized. Samples 10GR06 (Paikon unit) and 10GR51 (Nea Zoi unit) have pyroclastic (tuffaceous) texture with fragments of plagioclase and quartz set in a cryptocrystalline groundmass. Most of the pillow and massive lavas of these rock-types have a porphyritic or glomeroporphyritic texture with PI ranging from 10 to 50. Phenocrysts are represented by plagioclase and clinopyroxene. The groundmass in porphyritic rocks includes cryptocrystalline, hypohyaline, hyaline, and subophytic varieties. Hyaline groundmass shows perlitic texture. Only pillowed andesite 10GR22 (Krania unit) show aphyric, hyaline texture. The basaltic andesite dyke 10GR21 displays coarse-grained, doleritic texture with altered plagioclase and clinopyroxene. All these rocks underwent severe alteration with re-crystallization of primary minerals into chlorite, clay minerals and calcite. A few samples have amygdals filled by calcite.

Amphibolites from the Liki unit have nematoblastic texture characterized by alternation of layers of hornblende and layers of plagioclase and quartz. Plagioclase is completely altered in sericite.

GEOCHEMISTRY

The description of the geochemistry of the samples studied in this paper will be mainly based on the elements virtually immobile during alteration and metamorphism (e.g., Beccaluva et al., 1979; Pearce and Norry, 1979). Generally, immobile elements include incompatible elements, such as Ti, P, Zr, Y, Sc, Nb, Ta, Hf, Th, middle (M-) and heavy (H-) REE, as well as some transition metals (e.g., Ni, Co, Cr, V). Light REE (LREE) may be affected by some mobilization during alteration. However, the good correlations between LREE and many immobile elements (not shown) indicate that these elements have been only slightly mobilized by the alteration. The following discussion will be made by distinguishing in rock-groups the geochemically different rocks variably occurring in the units studied in this paper.

Group 1

Group 1 rocks are represented by massive lava basalts and one microgabbro dyke from the Ano Garefi unit. These rocks have a clear alkaline nature (Table 2) evidenced by high Nb/Y ratios (1.34-1.68). They are characterized by relatively high TiO₂ (2.01-2.15 wt%), P₂O₅ (0.45-0.60 wt%), Zr (176-194 ppm), Y (21-38.8 ppm) and Ti/V ratios (55-73). In the discrimination diagrams in Figs. 5a, 6a these rocks plot in the field for alkaline within-plate basalts. Accordingly, the incompatible element patterns (Fig. 7a) are characterized by decreasing abundance, from Ba to Yb, which are comparable to those of typical within-plate alkali basalts (Sun and McDonough, 1989). These rocks display significant LREE enrichment with respect to HREE (Fig. 7b), which is exemplified by their La_N/Yb_N ratios ranging from 6.7 to 9.6. The La/Nb ratios (0.61-0.66) are also compatible with those of typical OIB (0.77; Sun and McDonough, 1989).

Group 2

Group 2 rocks are represented by one basaltic dyke from the Ano Garefi unit. This rock shows a subalkaline nature, having a Nb/Y ratios = 0.49. It is characterized by moderately high TiO₂ (1.53 wt%), P₂O₅ (0.28 wt%), Zr (92.8 ppm), Y (19.6 ppm) contents and Ti/V ratio (55). In the discrimination diagrams in Figs. 5a and 6a this rock plots in the field for E-MORBs. Its incompatible element pattern (Fig. 7a) displays decreasing abundance, from Th to Yb, as well as moderate enrichment in Th, Ta, and Nb, which are comparable to those of typical E-MORBs (Sun and McDonough, 1989). This rock displays moderate LREE enrichment with respect to HREE (Fig. 7b), as exemplified by a La_N/Yb_N ratio = 3.12.

Group 3

Group 3 rocks are represented by basaltic rocks cropping out in the Paikon, Krania, Mavrolakkos, Vrissi, and Nea Zoi units, as well as one amphibolite sample from the Liki unit, which derives from a basaltic protholith (Table 2). They consist of basalts and ferrobasalts. No chemical differences exist between samples from different units. Basalts have moderate to high TiO₂ (0.80-1.86 wt%), P₂O₅ (0.07-0.20 wt%), V (231-388 ppm), Zr (49-136 ppm) and Y (15-39 ppm) contents. Mg# ranges from 68.5 and 46.0 suggesting that Group 3 rocks represent lavas ranging from primitive to slightly differentiated. Ferrobasalts have comparatively higher TiO₂ (1.81-2.60 wt%), FeO_t (13.70-17.91 wt%), P₂O₅ (0.16-0.43 wt%), V (405-466 ppm), Zr (104-238 ppm) and Y (23-69 ppm) contents. The high FeO_t contents result in low Mg# (50.3-30.5). Many trace elements show similar contents in basalts and ferrobasalts (Table 2). Only Cr contents are comparatively higher in basalts (Cr = 141-429 ppm) with respect to ferrobasalts (Cr = 33-198 ppm). Nb, Hf, Ta, and Th contents are generally very low. Nonetheless, a rough tendency of increase of the contents of these elements from basalts to ferrobasalts can be observed (Table 2, Fig. 7c, e).

In general, the overall geochemical features of both basalts and ferrobasalts are similar to those of equivalent rocks generated at modern mid-ocean ridges (Sun and McDonough, 1989). Accordingly, the low Nb/Y ratios (0.07-0.23) testify for the sub-alkaline nature of these rocks. Both basalts and ferrobasalts show rather flat incompatible element patterns in the N-MORB-normalized (Sun and McDonough, 1989) diagrams in Fig. 7c, e. REE abundance

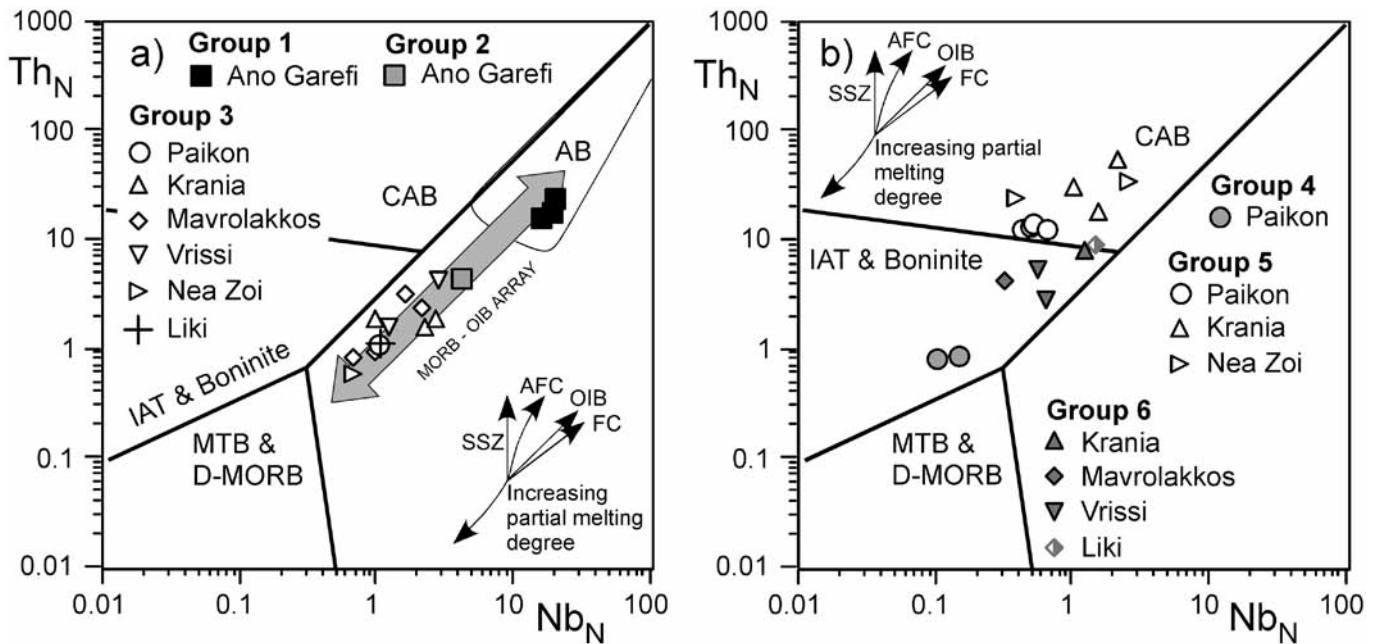


Fig. 5 - N-MORB normalized (Sun and McDonough, 1989) Th vs. Nb discrimination diagrams (Saccani, 2014) for volcanic and subvolcanic rocks from the Paikon unit and Almopias ophiolitic units. a) Groups 1-3 (subduction unrelated) rocks; b) Groups 4-6 (subduction related) rocks. Abbreviations: CAB- calc-alkaline basalt; IAT- island arc tholeiite; MORB- mid-ocean ridge basalt; AB- alkaline basalt; MTB- medium-Ti basalt; D-MORB- depleted MORB. The trends for compositional variations due to ocean island basalts-type (OIB) and supra-subduction zone type (SSZ) enrichments, fractional crystallization (FC) and assimilation-fractional crystallization (AFC) are shown.

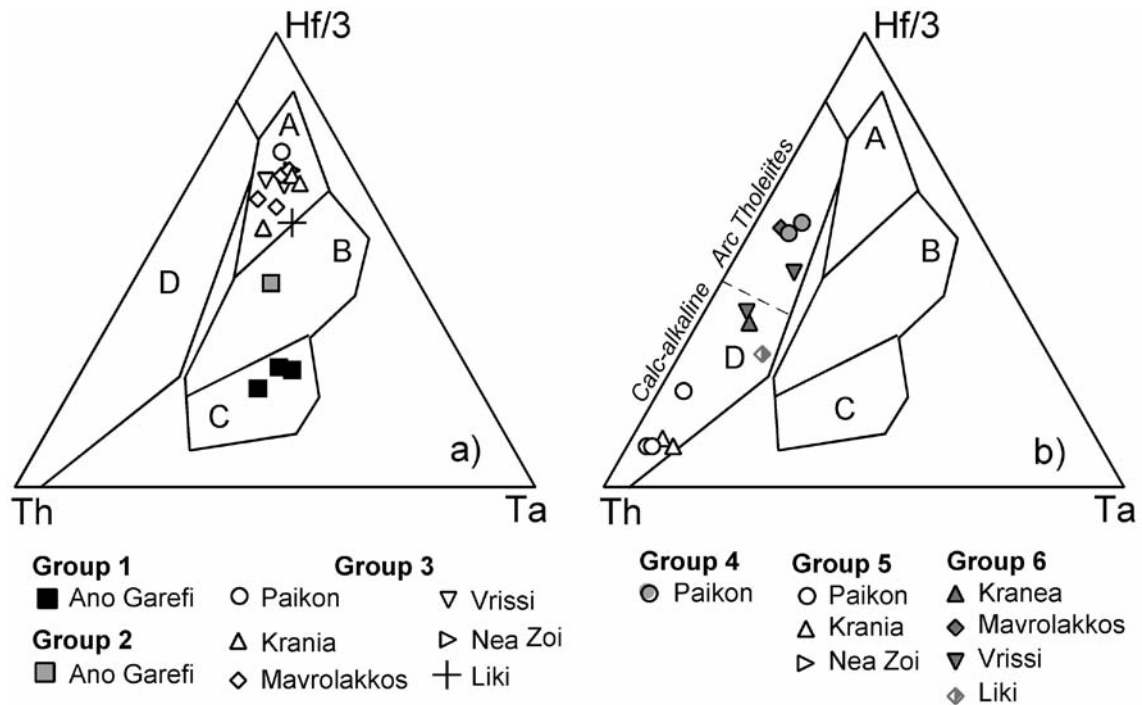


Fig. 6 - Th, Ta, Hf/3 discrimination diagrams (Wood, 1980) for volcanic and subvolcanic rocks from the Paikon unit and Almopias ophiolitic units. a) Groups 1-3 (subduction unrelated) rocks; b) Groups 4-6 (subduction related) rocks. Fields: A- normal mid-ocean ridge basalt; B- transitional mid-ocean ridge basalt and within-plate tholeiite; C- within-plate alkali basalt; D- volcanic arc basalt.

(Fig. 7d, f) varies from 6 to 35 times that of chondrite. All samples display profiles characterized by a general LREE depletion. Indeed, $(La/Sm)_N$ and $(La/Yb)_N$ range from 0.53 to 0.87 and from 0.48 to 1.07, respectively. Again, these ratios are similar in basalts and ferrobasalts. In the Th_N vs. Nb_N

discrimination diagram in Fig. 5a (Saccani, 2014) they plot along the MORB-OIB array. Basalts generally plot in the field for N-MORB, whereas ferrobasalts plot toward the field for E-MORB. In contrast, in the discrimination diagram in Fig. 6a (Wood, 1980) all samples plot in N-MORB field.

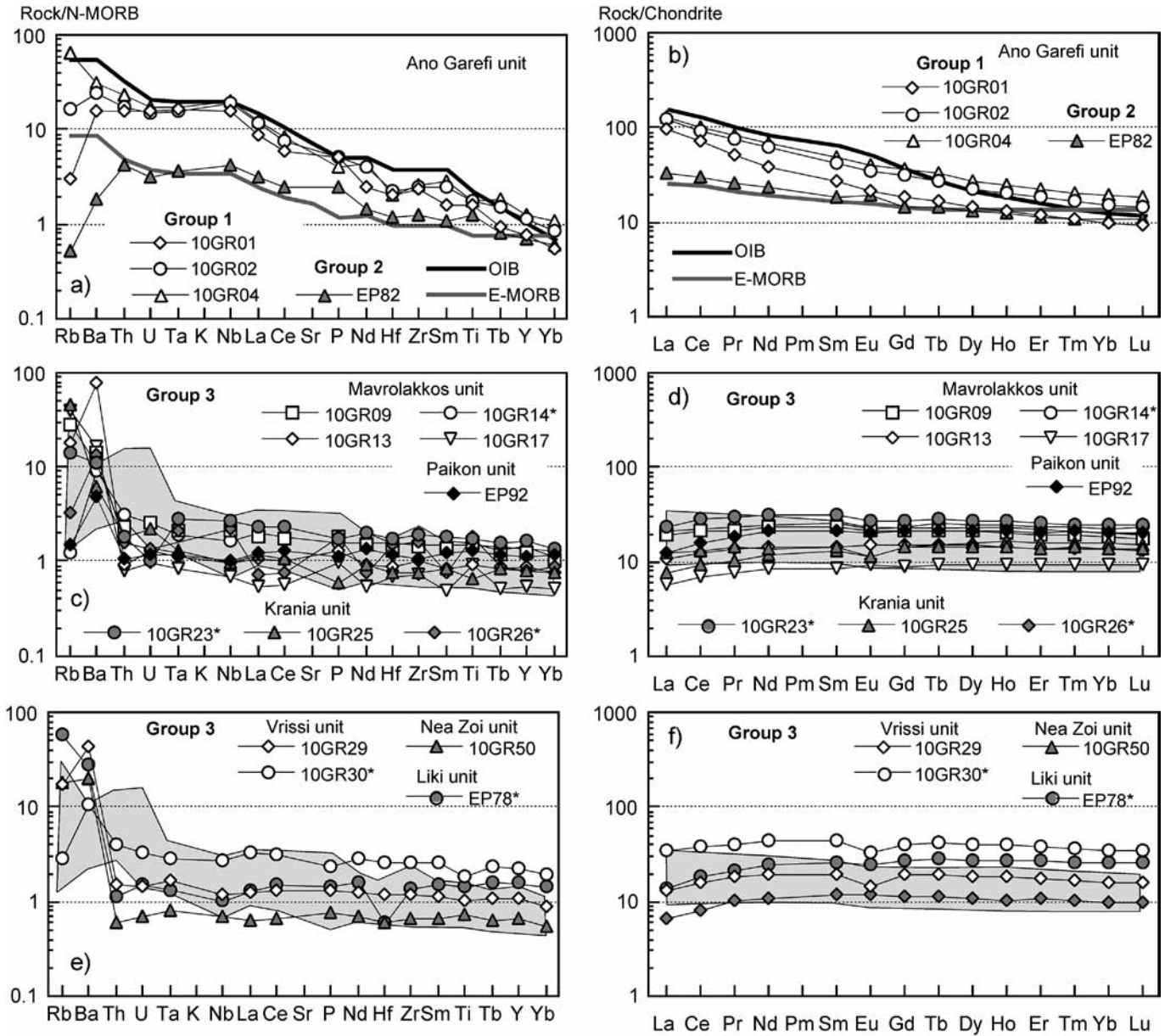


Fig. 7 - N-MORB normalized incompatible element patterns (a, c, e) and chondrite-normalized REE patterns (b, d, f) for Groups 1-3 (subduction unrelated) volcanic and subvolcanic rocks from the Paikon unit and Almopias ophiolitic units. * indicates Fe-basaltic rocks. The composition of typical alkaline ocean island basalt (OIB) and enriched-type mid-ocean ridge basalt (E-MORB), as well as the normalizing values are from Sun and McDonough (1989). The compositional variation of backarc basin basalts from the Guevgueli ophiolites (grey fields in panels e-f) is shown for comparison (data from Saccani et al., 2008a).

Group 4

Group 4 rocks are represented by basalts from the Paikon unit (Table 2). These rocks have distinctive very low TiO_2 (0.40-0.47 wt%), Zr (17-18 ppm) and Y (8 ppm) contents. In the diagram in Fig. 5b they plot in the field for boninites and IAT rocks. Nonetheless, based on their chondrite-normalized Dy content < 8.5 they can be classified as boninitic basalts (Saccani, 2014). Group 4 rocks are very depleted in incompatible elements, with high field strength elements (HFSE) ranging from 0.1 to 0.5 times N-MORB abundance (Fig. 8a). They show very depleted REE composition (Fig. 8b). REE patterns are characterized by LREE depletion with respect to both MREE and HREE with very low La_N/Sm_N (0.58-0.68) and La_N/Yb_N (0.28-0.33) ratios.

Group 5

Group 5 volcanic and subvolcanic rocks are represented by basalts, basaltic andesites, andesites, dacites and rhyolites from the Paikon, Krania, and Nea Zoi units (Table 2). Differentiated rocks are largely prevailing in volume with respect to basaltic rocks. Basaltic rocks are relatively poor in TiO_2 (0.84 wt%), Zr (47-85 ppm), and Y (16-33 ppm) but relatively rich in Al_2O_3 (14.91-16.88 wt%). Cr, Ni, and V contents are highly variable, whereas Mg# is very high (Table 2). Andesites, dacites and rhyolites contain low amounts of TiO_2 (0.23-0.82 wt%) and P_2O_5 (0.02-0.13 wt%). Likewise, Ni, Cr, and V are very low, except in samples EP91 (Paikon unit) and 10GR51 (Nea Zoi unit) where they are anomalously high. Compared to basaltic rocks, Zr (55-215 ppm) is higher, whereas Y (10-34 ppm) shows similar values. Mg# is very variable and it negatively correlated

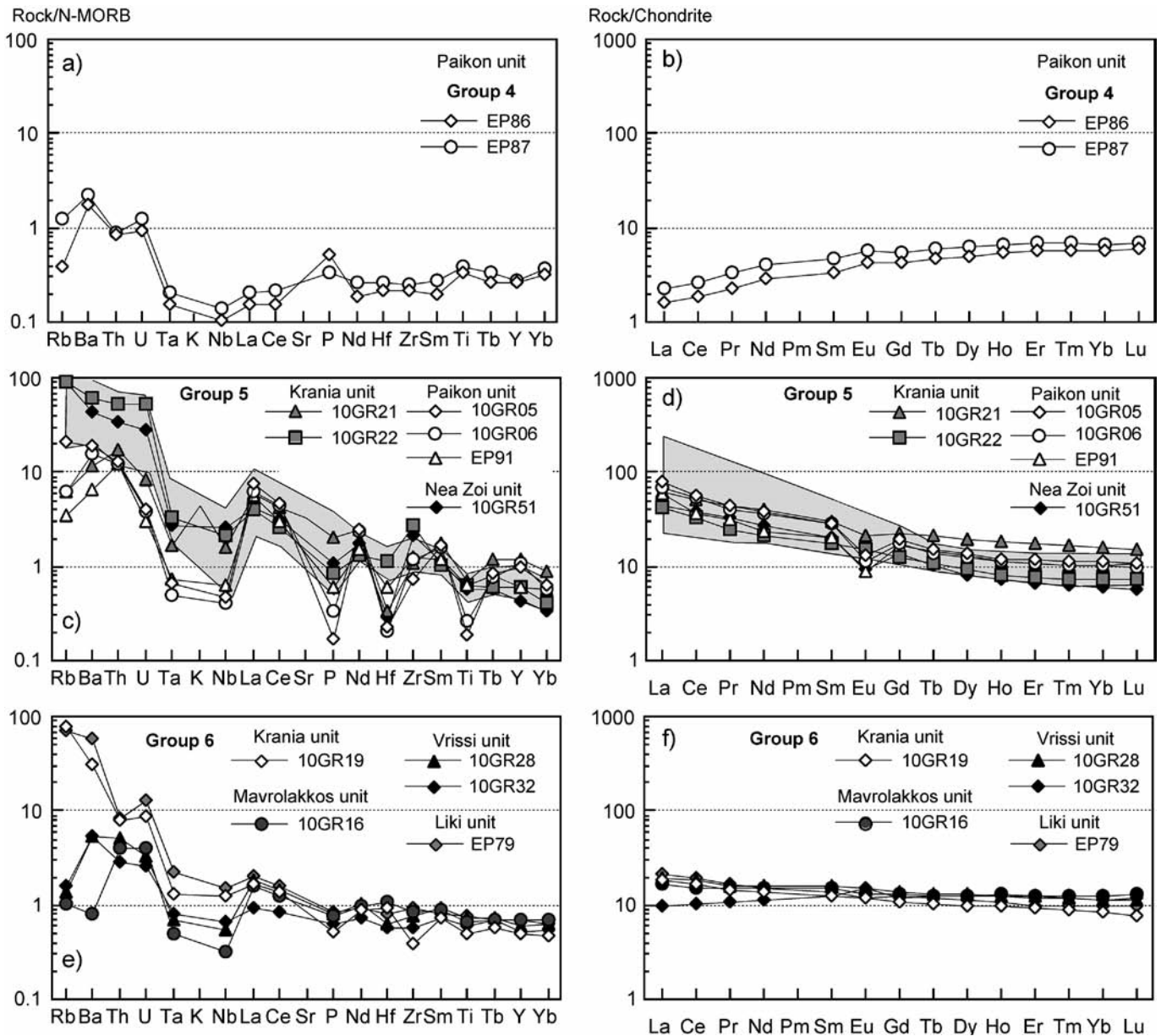


Fig. 8 - N-MORB normalized incompatible element patterns (a, c, e) and chondrite-normalized REE patterns (b, d, f) for Groups 4-6 (subduction related) volcanic and subvolcanic rocks from the Paikon unit and Almopias ophiolitic units. Normalizing values are from Sun and McDonough (1989). The compositional variations of calc-alkaline rocks from Guevgueli ophiolites (grey fields in panels c, d) are reported for comparison (data from Saccani et al., 2008a).

with Zr contents (not shown). However, no correlation is observed between Mg# and SiO₂ contents (not shown), suggesting that these samples underwent variable amounts of silica mobilization.

All Group 5 rocks have low Nb/Y ratios (0.03-0.51), which testify for their sub-alkaline nature. In the discrimination diagrams in Figs. 5b and 6b Group 5 rocks plot in the fields for CABs. Accordingly, in the FeO_T/MgO vs. SiO₂ discrimination diagram of Miyashiro (1974) (not shown) they plot in the field for calc-alkaline rocks. Incompatible and REE patterns (Fig. 8c, d) are consistent with these conclusions. In fact, as commonly observed in calc-alkaline rocks from volcanic arc settings, Group 5 rocks are characterized by Th and U enrichment and HFSE depletion, relative to N-MORB, with positive anomalies of Th, U, La, Ce and marked negative anomalies of Ta, Nb, P, Hf, and Ti.

REE display LREE/HREE enriched patterns (Fig. 8d), with La_N/Yb_N ratios ranging from 3.9 to 7.5. The CaO/Al₂O₃ ratios sharply decrease from basaltic rocks to andesites and dacites, whereas they slightly increase with decreasing Mg# (not shown) in the differentiated products. As observed by the petrographic analyses, this is consistent with the early crystallization of clinopyroxene with respect to plagioclase in basaltic rocks followed by massive crystallization of plagioclase in differentiated rocks. Enrichment of Th relative to Nb (Fig. 5b), as well as to Ta (Fig. 8c) suggests that Group 5 rocks are clearly influenced by an arc geochemical component (Pearce, 2008). In summary, based on their overall geochemical characteristics, Group 5 volcanic and subvolcanic rocks can be classified as a calc-alkaline rocks generated at destructive plate margin.

Group 6

Group 6 rocks are represented by basalts from the Krania and Vrissi units, as well as one andesite dyke from the Mavrolakkos unit and one amphibolite sample (from andesitic protolith) from the Liki unit (Table 2). Basalts are relatively poor in TiO_2 (0.60-0.77 wt%), P_2O_5 (0.06-0.08 wt%), Zr (29-48 ppm), and Y (12-20 ppm). In contrast, in the andesite and amphibolite samples TiO_2 (0.81-0.97 wt%), P_2O_5 (0.09-0.10 wt%), and Zr (63-70 ppm), contents are comparatively higher. Many elements (e.g., Al_2O_3 , Ni, Co, Cr, V) show very variable contents in both basaltic and andesitic samples. All Group 6 rocks show a clear sub-alkaline nature, as testified by low Nb/Y ratios (0.04-0.22). In the discrimination diagram in Fig. 5b these rocks plot in the field for IAT rocks, whereas in Fig. 6b they plot in the field for volcanic arc basalts, toward the field for low-K tholeiites (LKT). The N-MORB normalized incompatible element patterns are characterized by Th positive anomalies and Ta and Nb negative anomalies. However, in contrast to Group 5 rocks, they rocks do not show clear P, Hf, and Ti negative anomalies (Fig. 8e). The chondrite-normalized REE patterns are generally characterized by slightly LREE-enriched patterns (Fig. 8f), with La_N/Sm_N and La_N/Yb_N ratios ranging from 1.13 to 1.52 and from 1.24 to 2.21, respectively. Only sample 10GR32 (Vrissi unit) shows a slight LREE depletion with respect both MREE ($\text{La}_N/\text{Sm}_N = 0.77$) and HREE ($\text{La}_N/\text{Yb}_N = 0.84$). Likewise Group 5 rocks, the enrichment of Th relative to Nb and Ta (Figs. 5b, 8e) suggests that Group 6 rocks are clearly influenced by an arc geochemical component (Pearce, 2008). In summary, the overall geochemical characteristics of Group 6 rocks are very similar to those LKTs generated at destructive plate margin.

DISCUSSION

Tectono-magmatic significance of volcanic and subvolcanic rocks

It is commonly accepted that different rock associations in ophiolitic complexes provide major constraints for the recognition of the distinct phases of evolution of an oceanic basin (e.g., Beccaluva et al., 1979; Pearce, 1982). In fact, compositional differences between magma types in ophiolites are related to different source characteristics, which are associated, in turn, with distinct tectono-magmatic settings of formation. Beside the chemical variation due to fractional crystallization processes, distinct chemical compositions suggest that the different magmatic rock-types from the Paikon and Almopias units were originated from chemically distinct mantle sources. It can therefore be assumed that they were formed in distinct tectonic settings.

An estimation of the possible mantle sources of the different rock series from the Paikon and Almopias units can be obtained using incompatible elements such as Th and Nb. Therefore, partial melting modelings using Th and Nb abundance are presented in Fig. 9. Using Th vs. Nb plot has a double advantage: 1) the enrichment of Th relative to Nb is used to evaluate the chemical contribution from SSZ processes or crustal contamination, whereas the enrichment of Nb relative to Th is used to evaluate the chemical contribution from an OIB-type (plume type) component (Pearce, 2008; Saccani, 2014); 2) both Th and Nb behave similarly during partial melting in either spinel-facies or garnet-facies mantle. This allows the problem of possible melting in the spinel- or garnet-facies mantle (or a combination of both) to

be ruled out. Nonetheless, a rigorous quantification of the melting processes is not possible as the composition of the mantle sources are difficult to constrain. However, a semi-quantitative modeling of these elements can place some effective constraints.

Fig. 9a, b shows that Group 1 basalts from the Ano Garefi unit are compatible with low degrees of partial melting (2.5-5%) of an OIB-type source, whereas Group 2 basalt from the same unit is compatible with about 10% partial melting of a MORB-type source enriched by an OIB-type component. This implies that the alkaline volcanic sequence of the Ano Garefi unit was formed from a mantle source strongly influenced by plume-type components. The Group 2 basalt showing E-MORB chemistry represents a dyke cutting peridotites. Moreover, Migiros and Galeos (1987) described the occurrence of MORBs in the Ano Garefi unit. A clear interpretation of the tectono-magmatic setting of formation of the Ano Garefi unit cannot be made due to the scarcity of data. Alkaline rocks associated with transitional basalts and sub-alkaline E-MORBs are widespread in the Hellenide ophiolites, particularly in the sub-ophiolitic mélanges of both External and western Almopias ophiolites (e.g., Pe-Piper and Panagos, 1990; Pe-Piper and Kotopouli, 1991; Jones and Robertson, 1991; Capedri et al., 1997; Pe-Piper, 1998; Saccani et al., 2003a; 2003b; 2008b; Saccani and Photiades, 2005; Bortolotti et al., 2009; Chiari et al., 2012). These rocks always show ages ranging from Early to Late Triassic. In the lack of any age data it can only be postulated that the Ano Garefi volcanic sequence represent Triassic oceanic crust formed in off-axis settings and/or an the ocean-continent transition zone.

The Th-Nb composition of Group 3 primitive basalts is compatible with 10-20% partial melting of a depleted MORB mantle source (DMM, Workman and Hart, 2005) (Fig. 9c). Group 3 rocks can thus be interpreted as N-MORB type rocks generated from a sub-oceanic mantle sources, with no influence from enriched OIB-type material or subduction-related components. Therefore, Group 3 rocks were most likely generated at mid-ocean ridge setting. Alternatively, N-MORBs without any subduction-related chemical influence may originate in mature backarc basin settings.

Group 4 basalts show clear boninitic-type chemistry. The model in Fig. 9d shows that they are compatible with high degrees of partial melting (20-30%) of a depleted harzburgitic source, which underwent limited enrichment by SSZ fluids. According to Stern and Bloomer (1992), these basalts may therefore have formed in a forearc tectonic setting during subduction initiation.

Group 5 rocks have LREE-enriched patterns (Fig. 8d) and depletions in Nb, Ta, P, Hf, and Ti (Fig. 8c). Group 6 rocks also show significant Nb and Ta depletion, but they can be distinguished from Group 5 rocks because of their lower P, Hf, and Ti depletion (Fig. 8e), as well as lower LREE/HREE enrichment (Fig. 8f). Both Group 5 and Group 6 rocks have compositions, which clearly indicate imprints of subduction-related processes (Pearce, 2008). However, the marked enrichments in Th compared to Nb, as well as in LREE, shown by Group 5 rocks, when compared to Group 6 rocks, suggest that the mantle sources of Group 5 rocks were metasomatized by subduction-related fluids and/or continental crust components to a larger extent with respect to those of Group 6 rocks. Accordingly, in the model shown in Fig. 9e, the Th-Nb composition of Group 5 primitive basalts is compatible with 15-20% partial melting of a fertile

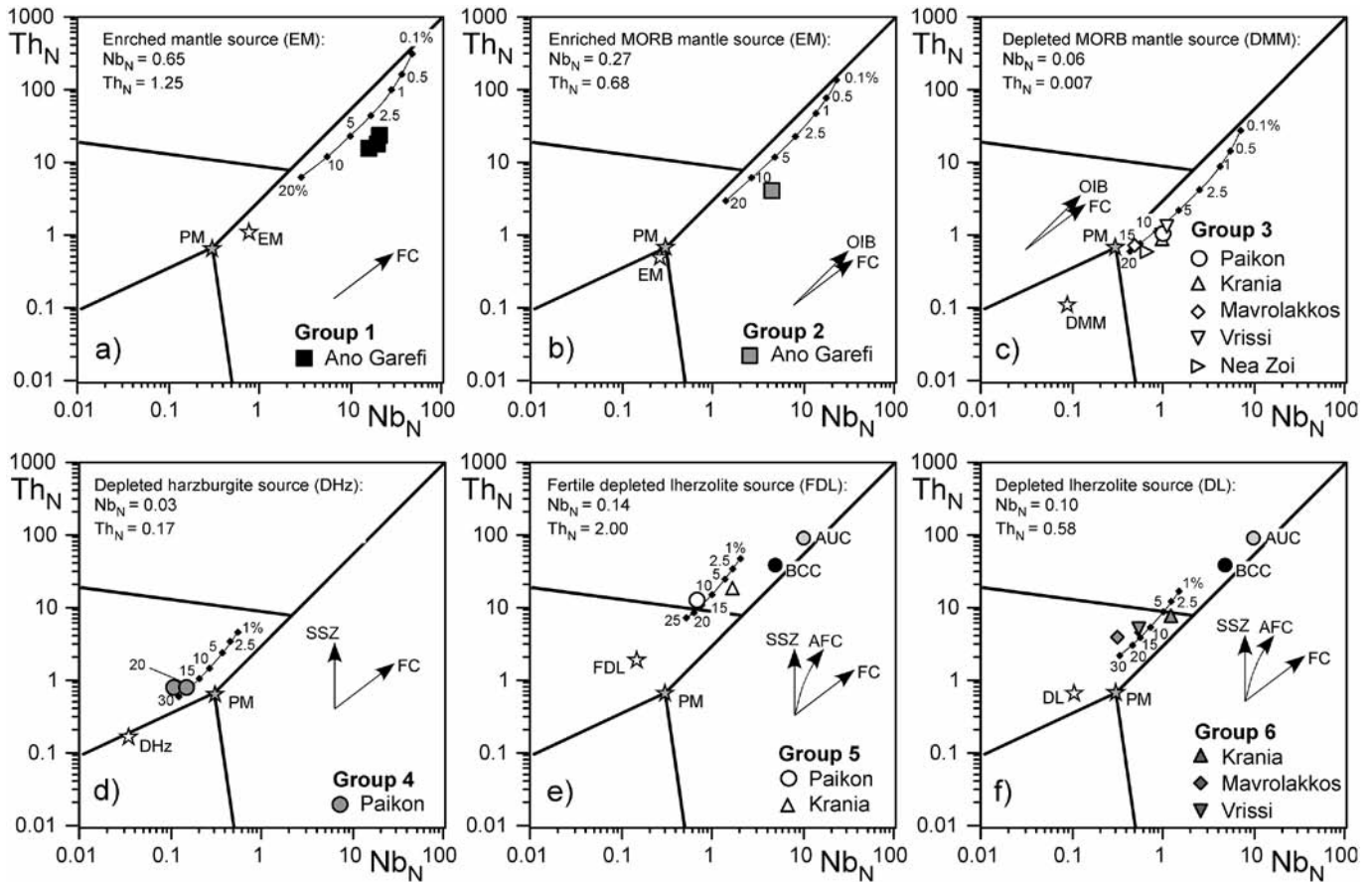


Fig. 9 - Plot of the Th_N vs. Nb_N compositional variations of the most primitive basalts of the different rock-groups from the Paikon and Almopias units, as well as melting curves for different mantle sources. Melting curves in panels a), b), and c) are calculated assuming non modal batch partial melting, whereas in panels d), e), and f) are calculated assuming non-modal fractional partial melting. Mantle source compositions in panels a) and b) are modified from Saccani et al. (2013); depleted MORB mantle (DMM) composition in panel c) is from Workman and Hart (2005); mantle compositions in panels d), e), f) are inferred based on Saccani et al. (2008c). The compositions of primordial mantle (PM, Sun and McDonough, 1989) bulk continental crust (BCC, Hofmann, 1988) and average upper crust (AUC, Taylor and McLennan, 1981) are also shown. Source modes and melting proportions in panels a), b), c) are from Thirlwall et al. (1994), whereas in panels d), e), f) are from Kostopoulos and Murton (1992). Partition coefficients are from McKenzie and O'Nions (1991). Arrows indicate the trends of variation for fractional crystallization (FC); ocean island basalt-type chemical component (OIB); supra-subduction type chemical component (SSZ); assimilation-fractional crystallization (AFC). See text for further explanations.

depleted lherzolite source significantly enriched in Th. Moreover, these rocks most likely experienced a chemical contribution from continental crust components. In contrast, the Th-Nb composition of Group 6 primitive basalts is compatible with various degrees of partial melting of a depleted lherzolite source enriched in Th (Fig. 9f). It can therefore be postulated that Jurassic Group 5 calc-alkaline rocks and Group 6 low-K tholeiitic rocks were originated in a continental margin volcanic arc setting or, alternatively, in an island arc setting characterized by complex polygenetic crust. Indeed, Bébien et al. (1994) demonstrated that the calc-alkaline magmatism in the Paikon sub-zone was developing during the Mid-Late Jurassic in a volcanic arc established onto the westernmost realm (present-day coordinated) of the Serbo-Macedonian continental basement. However, a different tectonic setting of formation can be postulated for the Late-Triassic Group 5 rocks now preserved in the ophiolitic mélangé of the Nea Zoi unit. In fact, Triassic calc-alkaline rocks crop out in many localities of the Hellenides (see Pe-Piper and Piper, 2002, pp. 94-95). According to Pe-Piper (1998), they were generated from the partial melting of the sub-continental mantle bearing subduction-related geochemical characteristics during the Triassic extensional tectonic

phase that caused the rifting of Gondwana. We can therefore conclude that the Late-Triassic calc-alkaline rocks in the Nea Zoi mélangé unit record the magmatic processes associated with the rifting of Gondwana that preceded the formation of the Vardar Ocean.

Occurrence and mutual relationships of the different rock-types in the Paikon and Almopias units

The Paikon and Almopias units are characterized by complex assemblages of rocks showing different magmatic affinities and that were formed in different tectonic settings. It is therefore necessary to sum up the occurrence of the various rock-types in each unit and to investigate their mutual relationships. Fig. 10 shows a summary of the occurrence of the different rock-types in both Paikon and Almopias units, which was compiled based on data presented in this paper coupled with literature data.

The Paikon unit is largely characterized by calc-alkaline rocks formed in a continental volcanic arc setting. Nonetheless, as already postulated by Bébien et al. (1994) this unit also include boninitic basalts and N-MORBs (Table 2). Unfortunately, due to the intense tectonization it was not possible to

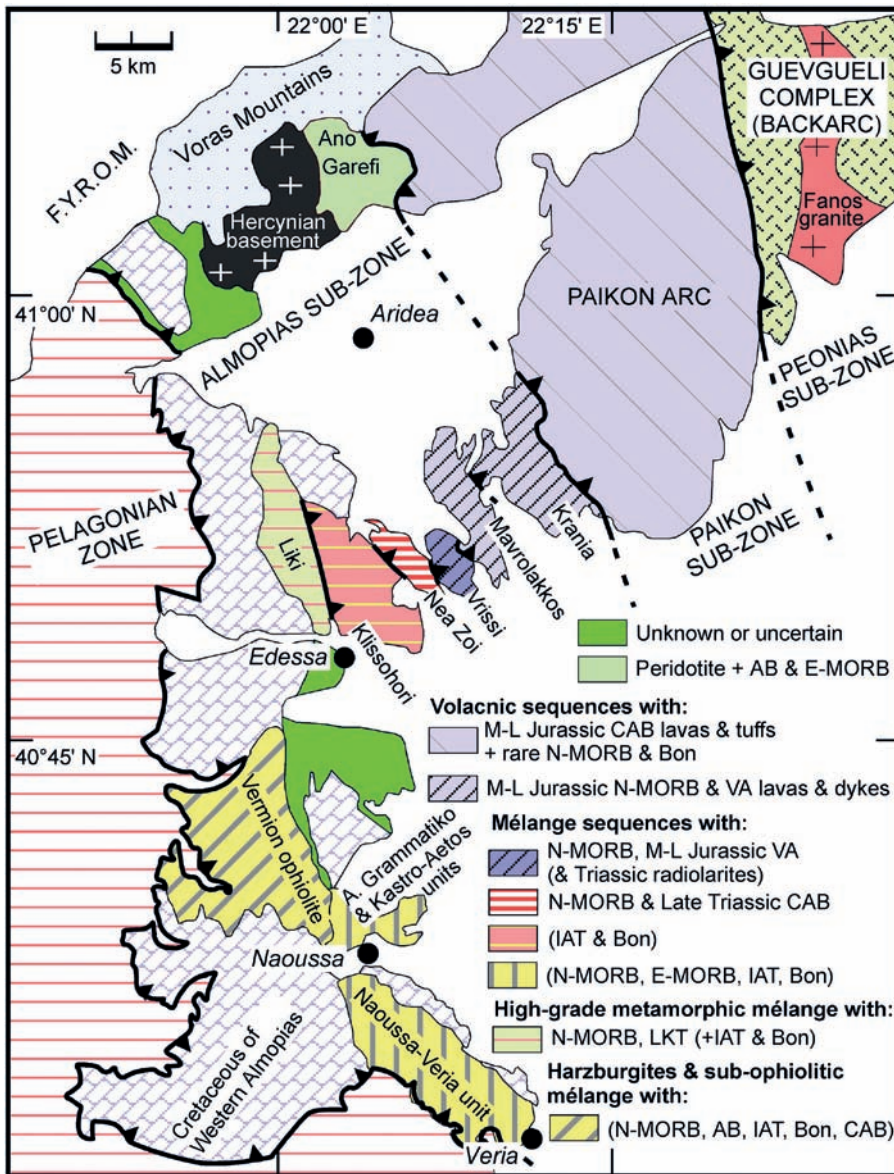


Fig. 10 - Sketch-map of the Vardar zone in the northern Greece (modified from Fig. 91 in Pe-Piper and Piper, 2002 and Saccani et al., 2008b) resuming the distribution of rocks with different magmatic affinities in the Paikon and Almopias units. Based on data presented in this paper, as well as literature data (Mercier and Vergély, 1972; Bijon, 1982; Staïs et al, 1990; De Wever, 1995; Sharp and Robertson, 1994; Saccani et al., 2008a). Parentheses indicate when literature data are used (see also text for details). Abbreviations: M- Middle; L- late; AB- alkaline basalt; CAB- calc-alkaline; MORB- mid-ocean ridge basalt; N- normal-type; E- enriched-type; LKT- low-K tholeiite; VA- volcanic arc (including CAB and LKT); IAT- island arc tholeiite, Bon- boninite.

investigate the mutual relationships between these different rock-types (Table 1). Therefore, no reliable hypotheses about the significance of N-MORBs and boninitic rocks in the Paikon unit can be made. Nonetheless, our data confirm the interpretation of Bébien et al. (1994) who suggested that this unit represents a Middle-Late Jurassic volcanic arc developed onto the Serbo-Macedonian continental realm.

The Ano Garefi unit completely differs from the other eastern Almopias ophiolitic units, as it consists of alkaline basalts directly overlying the peridotites and E-MORB dykes intruded in peridotites. Unfortunately, no dating of these rocks can be made due to the lack of associated radiolarian cherts. Moreover, the previous interpretation of peridotites as mantle harzburgites (Migiros and Galeos, 1987) cannot either be confirmed or excluded due to the lack of reliable data. Therefore, the tectonic significance of the Ano Garefi peridotites cannot be straightforwardly constrained. Nonetheless, in contrast to previous interpretations (Migiros and Galeos, 1987), preliminary data on a few samples from Ano Garefi peridotites (Authors' work in progress) seem to indicate that, they are represented by ultramafic cumulates likely showing MORB-type parentage.

Sharp and Robertson (1994) described the Krania unit (eastern Almopias ophiolites) as composed of Tithonian MORB rocks. In contrast, our data indicate that the Krania unit (eastern Almopias ophiolites) includes a Middle-Late Jurassic (late Bajocian-late Kimmeridgian/early Tithonian) basaltic massive lavas formed at mid-ocean ridge setting, as well as calc-alkaline pillowed and massive lavas and dykes and LKT dykes, formed in a volcanic arc setting. The calc-alkaline sequence seems to crop out at the base of the N-MORB type massive lavas (Table 1). However, due to recent sedimentary cover, the mutual relationships between these two different magmatic series cannot be verified. Moreover, the calc-alkaline series cannot be dated due to the lack of associated radiolarian cherts. Nonetheless, field observation seems to indicate that these two magmatic series are associated through a tectonic contact.

The Mavrolakkos unit (eastern Almopias ophiolites) consists of basalts showing N-MORB affinity, which crop out as massive lava flows and sheeted dykes (Table 1). Massive lavas are crosscut by basaltic and ferrobasic dykes also showing N-MORB affinity. Although dating of this unit by radiolarian biostratigraphy was not possible, these data are in

agreement with previous literature data. In fact, this unit was previously interpreted as a MORB-type volcanic sequence of Middle-Late Jurassic age (Staïis et al., 1990; Sharp and Robertson, 1994; De Wever, 1995). Nonetheless, our new data show that MORB lavas are crosscut by an andesitic dyke showing LKT affinity. This implies that the MORB-type Mavrolakkos volcanic sequence was also affected by contemporaneous or slightly younger volcanic arc magmatism.

Staïis et al. (1990) described the Vrissi unit (central Almopias ophiolites) as a *mélange* unit made up of (from bottom to top) Triassic radiolarian cherts tectonically overlain by a terrigenous sequence including shales with Late Cretaceous limestone lenses. Our data show that the volcanic section sampled in the Vrissi unit consists (from bottom to top) of basaltic and ferrobasaltic massive lava flows with N-MORB affinity overlain by LKT pillow lavas topped, in turn, by middle Callovian/early Oxfordian-late Kimmeridgian/early Tithonian (Middle-Late Jurassic) radiolarian cherts. The relationships between N-MORB and LKT lavas cannot clearly be seen in the field. Nonetheless, field evidence suggests that a major tectonic contact between these rock types is likely absent. Therefore, we suppose that they are possibly separated by a minor fault. In any case, the whole N-MORB sequence is crosscut by an LKT basaltic dyke. Likewise the Mavrolakkos unit (and possibly, the Krania unit), the studied volcanic section in the Vrissi unit clearly shows evidence for a MORB-type oceanic crust that was affected by younger volcanic arc magmatism.

The volcanic section sampled in the Nea Zoi unit (central Almopias ophiolites) includes N-MORB lavas, calc-alkaline rhyolites and basalts and Late Triassic (early Carnian-middle Norian) radiolarites. Mercier and Vergély (1972) have shown that this unit consists of a strongly foliated *mélange* unit. However, the volcanic section studied in this paper does not show foliation. We can therefore conclude that the Nea Zoi unit includes both foliated and non-foliated rocks.

The Liki unit (central Almopias ophiolites) includes basalts with N-MORB affinity and andesites with LKT affinity both metamorphosed under amphibolite facies conditions. No mutual relationships between these two different rock-types can be established. Moreover, Bijon (1982) described the occurrence of basalts with IAT affinity locally associated with felsic rocks and mafic lavas of boninitic affinity.

The Almopias ophiolites within the regional framework of the Vardar ophiolites

The new data presented herein, as well as previous literature data indicate that the Almopias ophiolitic units show a complex combination of different metamorphic, litho-stratigraphical, and age characteristics, which highlight some significant differences with respect to both External Ophiolites and the Internal Ophiolites of the Guevgueli Complex. Bortolotti et al. (2013) have recently proposed a new subdivision of the Albanide-Hellenide ophiolites based on a multidisciplinary approach (tectonics, stratigraphy, geochemistry, and biochronology). In other words, they proposed a subdivision that, regardless of the present-day position of these ophiolites, is essentially based on their genetic (including age) and tectonic significance. This subdivision includes six different types of “ophiolite-bearing” tectonic units: 1) sub-ophiolite *mélange* (SOM); 2) Triassic ocean-floor ophiolites (TOFO); 3) metamorphic soles (MES); 4) Jurassic fore-arc ophiolites (JFO); 5) Jurassic intra-oceanic-arc ophiolites (JIAO); 6) Jurassic back-arc basin ophiolites (JBO). The

first five units are found in the External Ophiolites and derived from the same oceanic obducted sheet, whereas JBO crops out in the Peonias sub-zone of the Internal Ophiolites. JFO and JIAO originated in two sectors of a unique intra-oceanic arc. In fact, in the JFO, MORB-type and intra-oceanic arc-type sequences are closely associated and often interlayered with each other, whereas mantle rocks are represented by depleted lherzolites and minor harzburgites (e.g., Hoeck et al., 2002; Saccani et al., 2011; Saccani and Tassinari, 2015). In contrast, in the JIAO, intrusive and volcanic sequences are largely characterized by intra-oceanic arc sequences and the mantle rocks are represented by harzburgites with abundant chromitites. Nonetheless, very minor intrusive rocks with MORB affinity locally occur within the SSZ sequences (e.g., Hoeck et al., 2002; Saccani et al., 2011; Saccani and Tassinari, 2015).

According to this subdivision, the western Almopias ophiolitic units in the Vermion range show some similarities with the External Ophiolites, as they include JIAO-type mantle harzburgites with chromitites associated with SOM units at their base. However, it should be noted that, in contrast to SOM units from the External Ophiolites, the sub-ophiolitic *mélange* in the Vermion ophiolites show intense deformation and metamorphism (Saccani et al., 2008b). The central Almopias ophiolites in the Naoussa and Veria areas (Fig. 10) show close similarities with the SOM units of the External Ophiolites. The only difference is represented by the abundant occurrence of tectonic slivers of volcanic rocks showing IAT affinity, which have not so far been documented in the External Ophiolite SOM units.

The Liki, Nea Zoi, and Vrissi units of the central Almopias ophiolites, though representing ophiolitic *mélange* units do not properly fit in the SOM type of Bortolotti et al. (2013). For instance, the Liki unit, though showing some similarities with SOM, underwent high-grade metamorphism and deformation under amphibolite-facies condition. Similar to some SOM units in the External Ophiolites (e.g., Capedri et al., 1997; Bortolotti et al., 2009), the Nea Zoi unit incorporates N-MORBs and Late Triassic calc-alkaline rocks. However, it includes two types of ophiolitic *mélanges*: one with tuffite matrix and another one with metabasite matrix and it is in part strongly foliated (Mercier and Vergély, 1972). Also these features have not so far been described in the SOM units in the External Ophiolites. The Vrissi unit, beside Triassic radiolarites (Staïis et al., 1990), includes an incomplete volcanic sequence (used here according to the ophiolite classification of Dilek and Furnes, 2011) consisting of N-MORB type volcanics associated with and crosscut by Middle-Late Jurassic (middle Callovian/early Oxfordian-late Kimmeridgian/early Tithonian) arc-arc-type volcanic rocks and dykes. No similar volcanic sequences have so far been documented in the SOM units from the External Ophiolites.

Also the eastern Almopias volcanic units do not fit in the Bortolotti et al. (2013) subdivision. The Mavrolakkos unit consists of N-MORB type sheeted dykes, lavas, and individual dykes of Middle-Late Jurassic age (Staïis et al., 1990; Sharp and Robertson, 1994; De Wever, 1995), which is crosscut by dykes showing volcanic arc affinity. The Krania unit consists of Middle-Late Jurassic (our data and Sharp and Robertson, 1994) N-MORB type basaltic rocks tectonically associated with calc-alkaline volcanics and dykes. In the External ophiolites, N-MORB volcanic rocks either cross cut by volcanic arc-type dikes or tectonically associated with calc-alkaline volcanics have not so far been described.

The Ano Garefi unit represents another peculiarity of the Almopias ophiolites, as it totally differs from the other ophiolitic units in the Almopias sub-zone, as well as from those of the External Ophiolites. In fact, no occurrence of a dyke-lava series showing alkaline affinity directly overlying harzburgitic tectonites, which are, in turn, cut by basaltic dykes showing E-MORB has so far been documented elsewhere in the Hellenides. Nonetheless, in the assumption that alkaline basalts are Triassic in age (see previous section) they may correlate with the TOFO units of the External Ophiolites, though no TOFO units associated with peridotites have so far been described. For this reason, the nature and chemistry of peridotites and the eventual existence of any genetic relationships with the overlying basaltic rocks need to be investigated in detail and will be the object of future investigation. Although not favoured in this paper, the hypothesis that the Ano Garefi alkaline volcanic sequence do not correlate with the TOFO-type, but was formed in Late Jurassic-Early Cretaceous times cannot be excluded. Basalts are locally interbedded with shales and limestones containing detrital chromite, which suggests provenance from the Jurassic SSZ-type depleted harzburgites and associated chromitites (Migiros and Galeos, 1987). According to these authors, this could imply that Jurassic SSZ-type harzburgites were uplifted and eroded when shales were deposited, supporting thus a Late Jurassic or younger age for these rocks. In fact, exposure of SSZ peridotites during Late Jurassic-Early Cretaceous times is documented in the western Almopias of the Vermion range by Fe-Ni laterites unconformably covering mantle harzburgites (Photiades et al., 1998; Saccani et al., 2008b). The possible formation of the Ano Garefi ophiolite during Late Jurassic-Early Cretaceous has already been postulated (Sharp and Robertson, 2006, p. 406, Fig. 21a). However, in this hypothesis, the main problem is to explain a Late Jurassic-Early Cretaceous activation of an OIB-type, enriched mantle source along the eastern margin of the Almopias sub-zone; that is, in a tectonic setting largely dominated by subduction below a continental margin.

Compared with the JBO-type of Bortolotti et al. (2013), none of the Almopias sub-zone units fit in this ophiolitic variety. In fact, JBO from the Peonias sub-zone are characterized by Middle and Late Jurassic (Danelian et al., 1996; Kukoč et al., 2015) volcanic sequences where calc-alkaline rocks are associated with backarc basin basalts showing clear subduction zone influence (i.e., Th and LREE enrichment coupled with Nb depletion, Saccani et al., 2008a). In contrast, in the central and eastern Almopias units Middle-Late Jurassic calc-alkaline rocks are associated with typical N-MORB rocks showing no evidence of subduction zone influence.

A major point arising from this paper is the occurrence in the central and eastern Almopias ophiolitic units of incomplete volcanic sequences with N-MORB lavas associated with volcanic arc-type lavas and/or intruded by volcanic arc-type dykes.

Our preliminary data do not allow a clear geodynamic model for explaining the almost coeval formation of MORB-type and volcanic arc-type magmatisms in the same area to be hypothesized. Several hypotheses can be taken into account. The partial melting of uprising primitive mantle producing MORB-type magmatism close to a volcanic arc setting can be related to several different tectonic mechanisms (i.e., strike-slip, leaky transform, slab windows tectonics). Ferrière et al. (2012) suggested that the rollback toward the west of the Late Jurassic subducting slab under the Paikon arc could be responsible for the development of an oceanic

crust younger than that recorded in the External ophiolites.

Age data show that the Middle-Late Jurassic volcanic arc magmatism recorded in the central and eastern Almopias units is correlative of that of the Paikon arc (Brown and Robertson, 2004), as well as that in the Guevgueli backarc complex (Saccani et al., 2008a). Our data show that not all the Almopias ophiolitic units and the Paikon arc unit can correlate with other ophiolitic units in the Dinaride-Hellenide belt, originated in the ocean, far from arc and back-arc settings. Schmid et al. (2008) have suggested that the eastern Vardar ophiolites could extend into the South Apuseni - Transylvanian ophiolitic belt in Romania (Fig. 1) (Bortolotti et al., 2002a; Ionescu et al., 2009; Ionescu and Hoeck, 2010). Schmid et al. (2008) also noted that the eastern Vardar ophiolitic belt does not extend along the Sava Zone in the Dinarides. The South Apuseni - Transylvanian ophiolites are indeed represented by Middle Jurassic N-MORB type oceanic crust underlying Late Jurassic calc-alkaline volcanics and also include some granites (Bortolotti et al., 2002a; 2004b; Nicolae and Saccani, 2003). Schmid et al. (2008) based their conclusion on the similarity between the South Apuseni - Transylvanian ophiolites and the Guevgueli ophiolites in northern Greece. According to these Authors, similar to the Guevgueli ophiolites, volcanic arc igneous rocks are only slightly younger than the surrounding MORB-type ophiolites, which they intrude. Nonetheless, in contrast to the South Apuseni - Transylvanian ophiolites, the Guevgueli ophiolites were formed in a backarc setting and instead of MORB-type oceanic crust they consist of BABB volcanic sequences (Saccani et al., 2008a). However, the conclusion of Schmid et al (2008) could still be valid. In fact, based on rock association and age of the eastern Almopias ophiolites and Paikon unit, we suggest that they could correlate with the South Apuseni - Transylvanian ophiolites. However, due to the complexity of the Almopias and Paikon units, many issues about their geodynamic significance within the Vardar zone remain unsolved. Therefore, a detailed investigation of these units will be carried out in future studies.

CONCLUSIONS

The Almopias and Paikon sub-zones in northern Greece represent the westernmost part of the Vardar area. The Almopias sub-zone consists of several ophiolite-bearing units, whereas the Paikon sub-zone includes volcanic units, which have been interpreted as formed at continental volcanic arc setting. Petrological and biostratigraphic studies carried out on volcanic rocks and associated radiolarian cherts provide new constraints for the interpretation of the Almopias and Paikon units, as summarized as follows.

(1) As already described in previous literature, the Paikon volcanic units largely consists of calc-alkaline volcanic rocks with very minor N-MORBs and boninites. Our data, therefore confirm that the Paikon volcanics have originated in a volcanic arc setting developed during the Middle to Late Jurassic times on the westernmost realm of the European plate.

(2) The Almopias ophiolitic units show a complex combination of different metamorphic, litho-stratigraphical, and age characteristics. The Liki, Nea Zoi, and Vrissi units of the central Almopias sub-zone consist of ophiolitic mélange units, whereas the Mavrolakkos and Krania units in the eastern Almopias sub-zone consist of volcanic sequences. The Liki unit underwent high-grade metamorphism and deformation under amphibolite-facies condition and includes

rocks showing N-MORB and LKT affinities. The Nea Zoi unit incorporates N-MORBs of unknown age and Late Triassic calc-alkaline rocks. The Vrissi unit includes an incomplete volcanic sequence consisting of N-MORB type volcanics linked with and crosscut by Middle-Late Jurassic arc-type volcanic rocks and dykes. The Mavrolakkos unit consists of N-MORB type sheeted dykes, lavas, and individual dykes series, which is crosscut by dykes showing volcanic arc affinity. The Krania unit consists of Middle-Late Jurassic -MORB type series tectonically associated with calc-alkaline volcanics and dykes. The Ano Garefi unit (eastern Almopias) completely differs from the other Almopias units as it consists of a dyke-lava series showing alkaline affinity directly overlying serpentinitized peridotites, which are, in turn, cut by basaltic dykes showing E-MORB. This unit may represent a fragment of Triassic oceanic crust formed at the ocean-continent transition zone.

(3) A major point arising from our data is the occurrence in the Almopias ophiolitic units of incomplete Middle-Late Jurassic volcanic sequences with N-MORB affinity associated with overlying volcanic arc-type lavas and/or intruded by volcanic arc-type dykes.

(4) Our data show that not all Almopias ophiolitic units, correlate with other ophiolitic units in the Dinaride-Hellenide belt, due to their peculiar paleogeographic setting, near the active Paikon arc. A possible correlation with the northernmost extension of the Vardar zone in the South Apuseni - Transylvanian ophiolitic belt in Romania could be hypothesized for some Almopias ophiolitic units.

ACKNOWLEDGEMENTS

The Italian Ministry of University is acknowledged for the financial support. Special thanks go to R. Tassinari and M. Bonora for their support with analytical techniques. Many thanks go to Michele Marroni and Paulian Dumitrica for their constructive reviews. Radiolarian micrographs were taken with a Zeiss EVO 15 of the MEMA, Dipartimento di Scienze della Terra, University of Florence and with a Philips XL20, Ivalsa, CNR.

REFERENCES

- Aubouin J., 1959. Contribution à l'étude géologique de la Grèce septentrionale: les confins de l'Épire et de la Thessalie. *Ann. Géol. Pays Hellén.*, 10, 483 pp.
- Baumgartner P.O., O'Dogherty L., Goričan Š., Dumitrica-Jud R., Dumitrica P., Pillecuit A., Urquhart E., Matsuoka A., Danelian T., Bartolini A., Carter E.S., De Wever P., Kito N., Marcucci M. and Steiger T.A., 1995a. Radiolarian catalogue and systematics of Middle Jurassic to Early Cretaceous Tethyan genera and species. In: P.O. Baumgartner, L. O'Dogherty, Š. Goričan, E. Urquhart, A. Pillecuit and P. De Wever (Eds.), *Middle Jurassic to Lower Cretaceous Radiolaria of Tethys: occurrences, systematics, biochronology*. *Mém. Géol. (Lausanne)*, 23: 37-685.
- Baumgartner P.O., Bartolini A., Carter E.S., Conti M., Cortese G., Danelian T., De Wever P., Dumitrica P., Dumitrica-Jud R., Goričan Š., Guex J., Hull D.M., Kito N., Marcucci M., Matsuoka A., Murchey B., O'Dogherty L., Savary J., Vishnevskaya V., Widz D. and Yao A., 1995b. Middle Jurassic to Early Cretaceous Radiolarian biochronology of Tethys based on Unitary Associations. In: P.O. Baumgartner, L. O'Dogherty, Š. Goričan, E. Urquhart, A. Pillecuit and P. De Wever (Eds.), *Middle Jurassic to Lower Cretaceous Radiolaria of Tethys: occurrences, systematics, biochronology*. *Mém. Géol. (Lausanne)*, 23: 1013-1048.
- Bébién J., 1983. L'association ignée de Guevgueli. *Ofioliti*, 8: 293-302.
- Bébién J. and Gagny C.I., 1979. Differentiation des magmas ophiolitiques: l'exemple du cortège de Guevgueli. In: A. Panayiotou (Ed.), *Ophiolites, Proceed. Intern. Ophiolite Symp.*, Cyprus. Geol. Survey Dept., Republic of Cyprus, p. 351-359.
- Bébién J., Baroz F., Capedri S. and Venturelli G., 1987. Magmatisme basiques associés a l'ouverture d'un bassin marginal dans les Hellénides Internes au Jurassique. *Ofioliti*, 12: 53-70.
- Bébién J., Ohnenstetter D., Ohnenstetter M. and Vergely P., 1980. Diversity of the Greek ophiolites: birth of oceanic basin in transcurrent systems. *Ofioliti, Spec. Iss.*, 2: 129-197.
- Bébién J., Platvoet B. and Mercier, J., 1994. Geodynamic significance of the Paikon Massif in the Hellenides: contribution of the volcanic rock studies. *Bull. Geol. Soc. Greece*, 30: 63-67.
- Beccaluva L., Ohnenstetter D. and Ohnenstetter M., 1979. Geochemical discrimination between ocean-floor and island-arc tholeiites-application to some ophiolites. *Can. J. Earth Sci.*, 16: 1874-1882.
- Bechon F., 1981. Caractères de tholéites abyssales des formations magmatiques basiques des unités orientales de la zone d'Almopias (Macedoine grecque). *C.R. Acad. Sci. Paris*, 292: 105-108.
- Bernoulli D. and Laubscher H., 1972. The palinspastic problem of the Hellenides. *Ecl. Geol. Helv.*, 65: 107-118.
- Bertrand J., Ferrière J. and Stais A., 1994. Données paléogéographiques et géochronologiques sur des laves des domaines vardariens de Péonias et d'Almopias (Hellénides orientales). *Bull. Géol. Soc. Grecque*, 30: 213-222.
- Bijon J., 1982. Géologie et géochimie des formations volcano-sédimentaires d'âge Jurassique supérieur et Crétacé de la région d'Edessa (Grèce, province de Pella). Thesis, Univ. Paris Sud, 192 pp.
- Bortolotti V. and Principi G., 2005. Tethyan ophiolites and Pangea break-up. *Isl. Arc*, 14: 442-470.
- Bortolotti V., Carras N., Chiari M., Fazzuoli M., Marcucci M., Nirta G., Principi G. and Saccani E., 2009. The ophiolite-bearing mélange in the Early Tertiary Pindos Flysch of Etolia (central Greece). *Ofioliti*, 34: 83-94.
- Bortolotti V., Carras N., Chiari M., Fazzuoli M., Marcucci M., Photiadis A. and Principi G., 2003. The Argolis Peninsula in the palaeogeographic and geodynamic frame of the Hellenides. *Ofioliti*, 28: 79-94.
- Bortolotti V., Chiari M., Kodra A., Marcucci M., Marroni M., Mustafa F., Prella M., Pandolfi L., Principi G. and Saccani E., 2006. Triassic MORB magmatism in the southern Mirdita Zone (Albania). *Ofioliti*, 31: 1-9.
- Bortolotti V., Chiari M., Marcucci M., Marroni M., Pandolfi L., Principi G. and Saccani E., 2004a. Comparison among the Albanian and Greek ophiolites: in search of constraints for the evolution of the Mesozoic Tethys ocean. *Ofioliti*, 29: 19-35.
- Bortolotti V., Chiari M., Marroni M., Pandolfi L., Principi G. and Saccani E., 2013. Geodynamic evolution of the ophiolites from Albania and Greece (Dinaric-Hellenic belt): One, two or more oceanic basins? *Int. J. Earth Sci.*, 102: 783-811, doi 10.1007/s00531-012-0835-7.
- Bortolotti V., Kodra A., Marroni M., Mustafa F., Pandolfi L., Principi G. and Saccani E., 1996. Geology and petrology of ophiolitic sequences in the Mirdita region (Northern Albania). *Ofioliti*, 21: 3-20.
- Bortolotti V., Marroni M., Nicolae I., Pandolfi L., Principi G. and Saccani E., 2002a. Geodynamic implications of Jurassic ophiolites associated with island-arc volcanics, South Apuseni Mountains, Western Romania. *Int. Geol. Rev.*, 44: 938-955.
- Bortolotti V., Marroni M., Nicolae I., Pandolfi L., Principi G. and Saccani E., 2004b. An update of the Jurassic ophiolites and associated calc-alkaline rocks in the South Apuseni Mountains (Western Romania). *Ofioliti*, 29: 5-18.
- Bortolotti V., Marroni M., Pandolfi L. and Principi G., 2005. Mesozoic to Tertiary tectonic history of the Mirdita ophiolites, northern Albania. *Isl. Arc*, 14: 471-493.

- Bortolotti V., Marroni M., Pandolfi L., Principi G. and Saccani E., 2002b. Interaction between mid-ocean ridge and subduction magmatism in Albanian ophiolites. *J. Geol.*, 110: 561-576.
- Bragin N.Y., 2007. Late Triassic radiolarians of Southern Cyprus. *Paleont. J.*, 41 (10): 951-1029.
- Brown S.A.M. and Robertson A.H.F., 2003. Sedimentary geology as a key to understanding the tectonic evolution of the Mesozoic-Early Cainozoic Paikon Massif, Vardar suture zone, N Greece. *Sedim. Geol.*, 160: 179-212.
- Brown S.A.M. and Robertson A.H.F., 2004. Evidence of Neotethys rooted within the Vardar suture zone from the Voras Massif, northernmost Greece. *Tectonophysics*, 381: 143-173.
- Capedri S., Toscani L., Grandi R., Venturelli G., Papanikolaou D. and Skarpelis N.S., 1997. Triassic volcanic rocks of some type-localities from the Hellenides. *Chem. Erde*, 57: 257-276.
- Chiari M., Baldanza A. and Parisi G., 2004a. Integrated stratigraphy (radiolarians and calcareous nannofossils) of the Jurassic siliceous sediments from Monte Kumeta (western Sicily, Italy). *Riv. It. Paleont. Stratigr.*, 110 (1): 129-140.
- Chiari M., Baumgartner P.O., Bernoulli D., Bortolotti V., Marcucci M., Photiades A. and Principi G., 2013. Late Triassic, Early and Middle Jurassic Radiolaria from ferromanganese-chert 'nodules' (Angelokastron, Argolis, Greece): evidence for prolonged radiolarite sedimentation in the Maliac-Vardar Ocean. *Facies*, 59: 391-424.
- Chiari M., Bortolotti V., Marcucci M., Photiades A. and Principi G., 2003. The Middle Jurassic siliceous sedimentary cover at the top of the Vourinos ophiolite (Greece). *Ofioliti*, 28 (2): 95-103.
- Chiari M., Bortolotti M., Marcucci M., Photiades A., Principi G. and Saccani E., 2012. Radiolarian biostratigraphy and geochemistry of the Koziakas Massif ophiolites (Greece). *Bull. Soc. Géol. Fr.*, 183 (4): 287-306.
- Chiari M., Cortese G., Marcucci M. and Nozzoli N., 1997. Radiolarian biostratigraphy in the sedimentary cover of the ophiolites of south-western Tuscany, Central Italy. *Ecl. Geol. Helv.*, 90: 55-77.
- Chiari M., Di Stefano P. and Parisi G., 2008. New stratigraphic data on the Middle-Late Jurassic biosiliceous sediments from the Sicilian basin, Western Sicily (Italy). *Swiss J. Geosci.*, 101: 415-429.
- Chiari M., Marcucci M. and Prela M., 2004b. Radiolarian assemblages from the Jurassic cherts of Albania: new data. *Ofioliti*, 29 (2): 95-105.
- Çollaku A., Cadet J.-P., Bonneau M. and Jolivet L., 1992. L'édifice structural de l'Albanie septentrionale: des éléments de réponse sur les modalités de la mise en place des ophiolites. *Bull. Soc. Géol. Fr.*, 163: 455-468.
- Danelian T., Lahsini S. and De Rafélis M., 2006. Upper Jurassic Radiolaria from the Vocontian basin of SE France. *Ecl. Geol. Helv.*, Suppl. Vol. 2: 35-47.
- Danelian T., Robertson A.H.F. and Dimitriadis S., 1996. Age and significance of radiolarian sediments within basic extrusives of the marginal basin Guevgueli Ophiolite (northern Greece). *Geol. Mag.*, 133: 127-136.
- Davis E., Jung D., Tsangalidis A. and Pavlopoulos A., 1988. Die Spilit-Keratophyr-Formation von Paikon (Z. Macedonia, Griechenland). [in Greek, German summary]. *Oryctos Plutos*, 53: 13-26.
- De Wever, 1995. Radiolarian overlying ophiolites of the Almopias domain (Macedonia, Greece). In: P.O. Baumgartner, L. O'Dogherty, Š. Goričan, E. Urquhart, A. Pillevuit and P. De Wever (Eds.), *Middle Jurassic to Lower Cretaceous Radiolaria of Tethys: occurrences, systematics, biochronology*. *Mém. Géol. (Lausanne)*, 23: 877-879.
- De Wever P., Sanfilippo A., Riedel W.R. and Gruber B., 1979. Triassic radiolarians from Greece, Sicily and Turkey. *Micropaleontology*, 25: 75-110.
- Dilek Y. and Furnes H., 2011. Ophiolite genesis and global tectonics: Geochemical and tectonic fingerprinting of ancient oceanic lithosphere: *Geol. Soc. Am. Bull.*, 123: 387-411, doi: 10.1130/B30446.1.
- Dilek Y., Furnes H. and Shallo M., 2007. Suprasubduction zone ophiolite formation along the periphery of Mesozoic Gondwana. *Gondw. Res.*, 11: 453-475.
- Dilek Y., Furnes H. and Shallo M., 2008. Geochemistry of the Jurassic Mirdita Ophiolite (Albania) and the MORB to SSZ evolution of a marginal basin oceanic crust. *Lithos* 100: 174-209.
- Doutsos R., Pe-Piper G., Boronkay K. and Koukouvelas I., 1993. Kinematics of the central Hellenides. *Tectonics*, 12: 936-953.
- Dumitrica P., Immenhauser A. and Dumitrica-Jud R., 1997. Mesozoic radiolarian biostratigraphy from Masirah ophiolite, Sultanate of Oman, Part 1. Middle Triassic, uppermost Jurassic and Lower Cretaceous spumellarians and multisegmented nassellarians. *Bull. Nat. Museum Nat. Sci.*, Taiwan, 9: 1-106.
- Ferrière J., Chanier F. and Ditbanjong P., 2012. The Hellenic ophiolites: eastward or westward obduction of the Maliac Ocean, a discussion. *Int. J. Earth Sci. (Geol. Rundsch.)*, 101: 1559-1580, doi 10.1007/s00531-012-0797-9.
- Goričan Š., Pavšič J. and Rožič B., 2012. Bajocian to Tithonian age of radiolarian cherts in the Tolmin Basin (NW Slovenia). *Bull. Soc. Géol. Fr.*, 183 (4): 369-382.
- Hauser M., Martini R., Burns S., Dumitrica P., Krystyn L., Matter A., Peters T. and Zaninetti L., 2001. Triassic stratigraphic evolution of the Arabian-Greater India embayment of the southern Tethys Margin. *Ecl. Geol. Helv.*, 94: 29-62.
- Hoeck V., Koller F., Meisel T., Onuzi K. and Kneringer E., 2002. The Jurassic South Albanian ophiolites: MOR- vs. SSZ-type ophiolites. *Lithos*, 65: 143-164.
- Hofmann A.W., 1988. Chemical differentiation of the Earth: the relationship between mantle, continental crust, and oceanic crust. *Earth Planet. Sci. Lett.*, 90: 297-314.
- Hull D.M., 1997. Upper Jurassic Tethyan and southern Boreal radiolarians from western North America. *Micropaleontology*, 43, Suppl. 2: 1-202.
- Ionescu C. and Hoeck V., 2010. Mesozoic ophiolites and granitoids in the Apuseni Mts. IMA2010 Field Trip Guide R02. *Acta Mineral.-Petrogr. Field guide series*, 20: 1-44.
- Ionescu C., Hoeck V., Tomek C., Koller F., Balintoni I. and Lucian B., 2009. New insights into the basement of the Transylvanian Depression (Romania). *Lithos*, 108: 172-191.
- Jach R., Djerić N., Goričan Š. and Reháková, D., 2014. Integrated stratigraphy of the Middle-Upper Jurassic of the Kržna Nappe, Tatra Mountains. *Ann. Soc. Geol. Polon.*, 84: 1-33.
- Jones G. and Robertson A.H.F., 1991. Tectono-stratigraphic evolution of the Mesozoic Pindos ophiolite and related units, north-western Greece. *J. Geol. Soc. London*, 148: 267-288.
- Kostopoulos D.K. and Murton B.J., 1992. Origin and distribution of components in boninite genesis: significance of the OIB component. In: L.M. Parson, B.J. Murton and P. Browning (Eds.), *Ophiolites and their modern oceanic analogues*. *Geol. Soc. London Spec. Publ.*, 60: 133-154.
- Krische O., Goričan Š. and Gawlich H.-J., 2014. Erosion of a Jurassic ophiolitic nappe-stack as indicated by exotic components in the Lower Cretaceous Rossfeld Formation of the Northern Calcareous Alps (Austria). *Geol. Carpath.*, 65 (1): 3-24.
- Kukoč D., Goričan Š., Košir A., Belak M., Halamić J. and Hrvatić H., 2015. Middle Jurassic age of basalts and the post-obduction sedimentary sequence in the Guevgueli Ophiolite Complex (Republic of Macedonia). *Int. J. Earth Sci. (Geol. Rundsch.)*, 104: 435-447.
- Lachance G.R. and Trail R.J., 1966. Practical solution to the matrix problem in X-ray analysis. *Can. Spectr.*, 11: 43-48.
- McKenzie D. and O'Nions R.K., 1991. Partial melt distributions from inversion of rare earth element concentrations. *J. Petrol.*, 32: 1021-1091.
- Mercier J., 1966a. Étude géologique des zones internes des Hellenides en Macédoine centrale (Grèce). *Ann. Géol. Pays Hellén.*, 20: 1-596.
- Mercier J., 1966b. Paléogéographie orogénèse, métamorphisme et magmatisme des zones internes des Hellenides en Macédoine (Grèce): vue d'ensemble. *Bull. Soc. Géol. France*, 8: 1020-1049.

- Mercier J., 1966c. Mouvements orogéniques et magmatisme d'âge Jurassique supérieur-Éocène dans les Zones Internes des Hellénides (Macédoine, Grèce). *Rev. Géogr. Phys. Géol. Dynam.*, (2), 8: 265-278.
- Mercier J., 1968. Étude géologique des zones Hellénides en Macédoine centrale (Grèce). *Ann. Géol. Pays Hellén.*, 20: 792 pp.
- Mercier J.-L. and Vergély P., 1972. Les mélanges ophiolitiques de Macédoine (Grèce): décrochements d'âge anté-Crétacé supérieur. *Z. dt. geol. Ges.*, 123: 469-489.
- Mercier J., Vergély P. and Bébien J., 1975. Les ophiolites hellénique «obductées» au Jurassique supérieur sont elles les vestiges d'un Océan téthysien ou d'une mer marginale péri-européenne? *C. R. S. Soc. Géol. France*, 17: 108-112.
- Migiros G. and Galeos A., 1987. Tectonic and stratigraphic significance of the Ano Garefi ophiolitic rocks, (Northern Greece). Ophiolites: oceanic crustal analogues. In: J. Malpas, E.M. Moores, A Panayiotou and C Xenophontos (Eds.), *Proceed. Symposium Troodos 1987. Memorial Univ., St. John's, NF, Canada*, p. 279-284.
- Miyashiro A., 1974. Volcanic rock series in island arcs and active continental margins. *Am. J. Sci.*, 274: 321-355.
- Nicolae I. and Saccani E., 2003. Petrology and geochemistry of the Late Jurassic calc-alkaline series associated to Middle Jurassic ophiolites in the South Apuseni Mountains (Romania). *Swiss J. Petrol.*, 83: 81-96.
- Nirta G., Bortolotti V., Chiari M., Menna M., Saccani E., Principi G. and Vannucchi P., 2010. Ophiolites from the Grammos-Arenes area, Northern Greece. Geological, paleontological and geochemical data. *Ophioliti*, 35 (2): 103-115.
- O'Dogherty L., Bill M., Goričan Š., Dumitrica P. and Masson H., 2006. Bathonian radiolarians from an ophiolitic mélange of the Alpine Tethys (Gets Nappe, Swiss-French Alps). *Micropaleontology*, 51: 425-485.
- O'Dogherty L., Carter E.S., Dumitrica P., Goričan Š., De Wever P., Hungerbühler A., Bandini A.N. and Takemura A., 2009a. Catalogue of Mesozoic radiolarian genera. Part 1: Triassic. *Geodiversitas*, 31: 213-270.
- O'Dogherty L., Carter E.S., Dumitrica P., Goričan Š., De Wever P., Bandini A.N., Baumgartner P.O. and Matsuoka A., 2009b. Catalogue of Mesozoic radiolarian genera. Part 2: Jurassic-Cretaceous. *Geodiversitas*, 31: 271-356.
- Pearce J.A., 1982. Trace element characteristics of lavas from destructive plate boundaries. In: R.S. Thorpe (Ed.), *Andesites*. Wiley, New York, p. 525-548.
- Pearce J.A., 2008. Geochemical fingerprinting of oceanic basalts with applications to ophiolite classification and the search for Archean oceanic crust. *Lithos*, 100: 14-48.
- Pearce J.A. and Norry M.J., 1979. Petrogenetic implications of Ti, Zr, Y, and Nb variations in volcanic rocks. *Contrib. Mineral. Petrol.*, 69: 33-47.
- Pe-Piper G., 1998. The nature of Triassic extension-related magmatism in Greece: Evidence from Nd and Pb isotope geochemistry. *Geol. Mag.*, 135: 331-348.
- Pe-Piper G. and Kotopouli C.N., 1991. Geochemical characteristics of the Triassic igneous rocks of the Island of Samos, Greece: *N. Jahrb. Mineral. Abhandl.*, 162: 135-150.
- Pe-Piper G. and Panagos A.G., 1989. Geochemical characteristics of the Triassic volcanic rocks of Evia: Petrogenetic and tectonic implications. *Ophioliti*, 14: 33-50.
- Pe-Piper G. and Piper D.J.W., 2002. The igneous rocks of Greece. The anatomy of an orogen. *Gebrüder Borntraeger, Berlin*, 573 pp.
- Photiades A., Skourtsis-Coroneou V. and Grigoris P., 1998. The stratigraphic and paleogeographic evolution of the Eastern Pelagonian margin during the Late Jurassic-Cretaceous interval (Western Vermion Mountain-Western Macedonia, Greece). *Bull. Geol. Soc. Greece*, 32: 71-77.
- Robertson A.H.F., 2012. Late Palaeozoic-Cenozoic tectonic development of Greece and Albania in the context of alternative reconstructions of Tethys in the Eastern Mediterranean region. *Int. Geol. Rev.*, 54: 373-454, doi: 10.1080/00206814.2010.543791.
- Robertson A.H.F. and Shallo M., 2000. Mesozoic-Tertiary tectonic evolution of Albania in its regional Eastern Mediterranean context. *Tectonophysics*, 316: 197-254.
- Saccani E., 2014. A new method of discriminating different types of post-Archean ophiolitic basalts and their tectonic significance using Th-Nb and Ce-Dy-Yb systematics. *Geosci. Front.*, <http://dx.doi.org/10.1016/j.gsf.2014.03.006>.
- Saccani E. and Photiades A., 2005. Petrogenesis and tectono-magmatic significance of volcanic and subvolcanic rocks in the Albanide-Hellenide ophiolitic mélanges. *Isl. Arc*, 14: 494-516.
- Saccani E. and Tassinari R., 2015. The role of MORB and SSZ magma-types in the formation of Jurassic ultramafic cumulates in the Mirdita ophiolites (Albania) as deduced from chromian spinel and olivine chemistry. *Ophioliti*, 40 (1): 37-56.
- Saccani E., Allahyari K., Beccaluva L. and Bianchini G., 2013. Geochemistry and petrology of the Kermanshah ophiolites (Iran): Implication for the interaction between passive rifting, oceanic accretion, and plume-components in the Southern Neo-Tethys Ocean. *Gondw. Res.*, 24: 392-411, <http://dx.doi.org/10.1016/j.gr.2012.10.009>.
- Saccani E., Beccaluva L., Photiades A. and Zeda O., 2011. Petrogenesis and tectono-magmatic significance of basalts and mantle peridotites from the Albanian-Greek ophiolites and sub-ophiolitic mélanges. New constraints for the Triassic-Jurassic evolution of the Neo-Tethys in the Dinaride sector. *Lithos*, 124: 227-242, doi: 10.1016/j.lithos.2010.10.009.
- Saccani E., Bortolotti V., Marroni M., Pandolfi L., Photiades A. and Principi G., 2008a. The Jurassic association of backarc basin ophiolites and calc-alkaline volcanics in the Guevgueli Complex (northern Greece): Implication for the evolution of the Vardar Zone. *Ophioliti*, 33: 209-227.
- Saccani E., Padoa E. and Photiades A., 2003b. Triassic mid-ocean ridge basalts from the Argolis Peninsula (Greece): new constraints for the early oceanization phases of the Neo-Tethyan Pindos basin. In: Y. Dilek and P.T. Robinson (Eds.), *Ophiolites in earth history: Geol. Soc. London Spec. Publ.*, 218: 109-127.
- Saccani E., Photiades A. and Beccaluva L. 2008c. Petrogenesis and tectonic significance of IAT magma-types in the Hellenide ophiolites as deduced from the Rhodiani ophiolites (Pelagonian zone, Greece). *Lithos*, 104: 71-84.
- Saccani E., Photiades A. and Padoa E., 2003a. Geochemistry, petrogenesis and tectono-magmatic significance of volcanic and subvolcanic rocks from the Koziakas mélange (Western Thessaly, Greece). *Ophioliti*, 28: 43-57.
- Saccani E., Photiades A., Santato A. and Zeda O., 2008b. New evidence for supra-subduction zone ophiolites in the Vardar zone from the Vermion massif (northern Greece): Implication for the tectono-magmatic evolution of the Vardar oceanic basin. *Ophioliti*, 33: 17-37.
- Sarić K., Cvetković V., Romer R.L., Christofides G. and Koroneos A., 2008. Granitoids associated with East Vardar ophiolites (Serbia, F.Y.R. of Macedonia and northern Greece): Origin, evolution and geodynamic significance inferred from major and trace element data and Sr-Nd-Pb isotopes. *Lithos*, 108: 131-150, doi:10.1016/j.lithos.2008.06.001.
- Schermer E.R., 1993. Geometry and kinematics of continental basement deformation during the Alpine orogeny, Mt. Olympus, Greece. *J. Struct. Geol.*, 15: 571-591.
- Schmid S.M., Bernoulli D., Fugenschuh B., Matenco L., Schefer S., Schuster R., Tischler M. and Ustaszewski K., 2008. The Alpine-Carpathian-Dinaridic orogenic system: correlation and evolution of tectonic units. *Swiss J. Geosci.*, 101: 139-183.
- Shallo M., 1992. Geological evolution of the Albanian ophiolites and their platform periphery. *Geol. Rund.*, 81: 681-694.
- Sharp I. and Robertson A., 1994. Late Jurassic - Lower Cretaceous oceanic crust and sediments of the eastern Almopias Zone, NW Macedonia (Greece); implications for the evolution of the eastern "Internal" Hellenides. *Bull. Geol. Soc. Greece*, 30: 47-61.

- Sharp I.R. and Robertson A.H.F., 2006. Tectonic-sedimentary evolution of the western margin of the Mesozoic Vardar Ocean: evidence from the Pelagonian and Almopias zones, northern Greece. In: A.H.F. Robertson and D. Mountrakis (Eds.), Tectonic development of the Eastern Mediterranean Region. Geol. Soc. London Spec. Publ., 260: 373-412.
- Staïs A., Ferrière J., Caridroit M., De Wever P., Clement B. and Bertrand J., 1990. Données nouvelles sur l'histoire ante-obduction (Trias-Jurassique) du domaine d'Almopias (Macédoine, Grèce). C.R. Acad. Sci. Paris, Série II, 310: 1275-1480.
- Staïs A. and Ferrière J., 1991. Nouvelles données sur la paléogéographie mésozoïque du domaine vardarien: les bassins d'Almopias et de Peonias (Macédoine, Hellénides internes septentrionales). Bull. Geol. Soc. Greece, 25: 491-507.
- Stern R.J. and Bloomer S.H., 1992. Subduction zone infancy: examples from the Eocene Izu-Bonin-Mariana and Jurassic California arcs. Geol. Soc. Am. Bull., 104: 1621-1636.
- Sun S.S. and McDonough W.F., 1989. Chemical and isotopic systematics of ocean basalts: Implications for mantle composition and processes. In: A.D. Saunders and M.J. Norry (Eds.), Magmatism in the ocean basins. Geol. Soc. London Spec. Publ., 42: 313-346.
- Taylor S.R. and McLennan S.M., 1981. The composition and evolution of the continental-crust - Rare-Earth element evidence from sedimentary-rocks. Philos. Trans. Royal Soc. London, 301: 381-399.
- Tekin U.K., 1999. Biostratigraphy and systematics of Late Middle to Late Triassic radiolarians from the Taurus Mountains and Ankara Region, Turkey. Geol. Paläont. Mitt., Innsbruck, 5: 1-296.
- Thirlwall M., Upton B.G.J. and Jenkins C., 1994. Interaction between continental lithosphere and the Iceland plume. Sr-Nd-Pb isotope geochemistry of Tertiary basalts, NE Greenland. J. Petrol., 35: 839-879.
- Vergély P., 1976. Origine "vardarienne" chevauchement vers l'ouest et rétrocharriage vers l'est des ophiolites de Macédoine (Grèce) au cours du Jurassique supérieur-Eocène. C.R. Acad. Sci. Paris, D 280: 1063-1066.
- Vergély P., 1984. Tectonique des ophiolites dans les Hellénides internes (déformations, métamorphismes et phénomènes sédimentaires): conséquences sur l'évolution des régions Téthysiennes occidentales. Thèse Etat, Univ. Paris-Sud, 611 pp.
- Vergély P. and Mercier J.-L., 2000. Données nouvelles sur les chevauchements d'âge post-Crétacé supérieur dans le massif du Paikon (zone de l'Axios-Vardar, Macédoine, Grèce): un nouveau modèle structural. C.R. Acad. Sci. Paris, Série IIA, 330: 555-561.
- Wood D.A., 1980. The application of a Th-Hf-Ta diagram to problems of tectonomagmatic classification and to establishing the nature of crustal contamination of basaltic lavas of the British Tertiary volcanic province. Earth Planet. Sci. Lett., 50: 11-30.
- Workman R.K. and Hart S.R., 2005. Major and trace element composition of the depleted MORB mantle (DMM). Earth Planet. Sci. Lett., 231: 53-72.

Received, September 25, 2014

Accepted, May 16, 2015

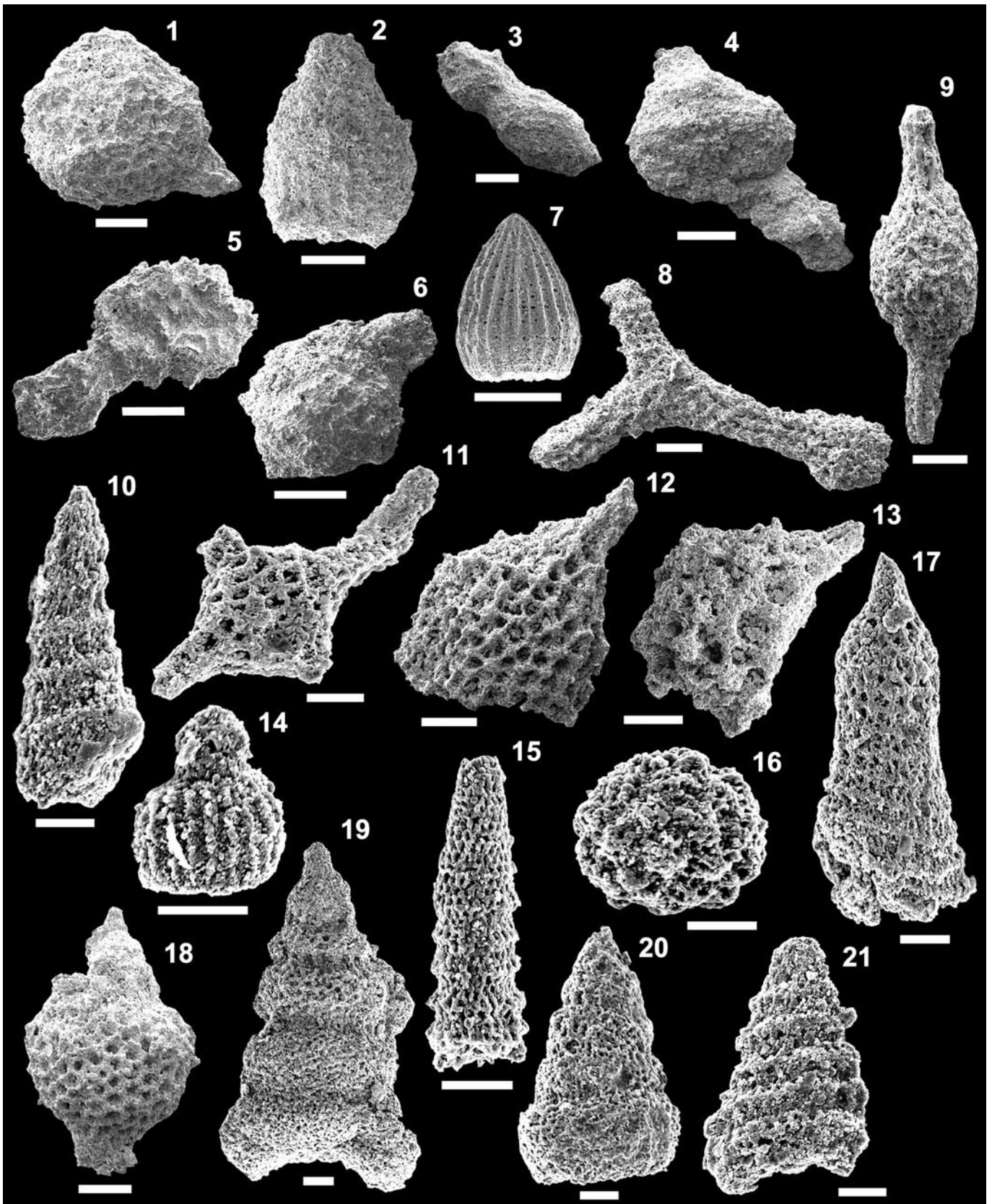


Plate 1 (scale bar = 50 μm) 1) *Capnuchosphaera* (?) sp., 10GR40. 2) *Nakasekoellus* sp., 10GR40. 3) *Capnuchosphaera constricta* (Kozur and Mock), 10GR42. 4) *Capnuchosphaera* (?) sp., 10GR42. 5) *Capnuchosphaera* sp., 10GR53. 6) *Capnuchosphaera* (?) sp. 10GR53. 7) *Archaeodictyomitra patricki* Kocher, 10GR27. 8) *Angulobracchia* sp. cf. *A. biordinalis* Ozvoldova, 10GR34. 9) *Archaeospongoprunum* sp. cf. *A. imlayi* Pessagno, 10GR34. 10) *Cingoloturris carpatica* Dumitrica, 10GR34. 11) *Emiluvia pentaporata* Steiger and Steiger, 10GR34. 12) *Emiluvia pessagnoii multipora* Steiger, 10GR34. 13) *Emiluvia* sp. cf. *E. sedecimporata* (Rüst), 10GR34. 14) *Eucyrtidiellum ptyctum* (Riedel and Sanfilippo), 10GR34. 15) *Praeparvicingula* sp., 10GR34. 16) *Praeconosphaera* sp. cf. *P. sphaeroconus* (Rüst), 10GR34. 17) *Ristola altissima altissima* (Rüst), 10GR34. 18) *Spinocapsa* (?) sp., 10GR34. 19) *Spongocapsula* sp. aff. *S. palmerae* Pessagno, 10GR34. 20) *Spongocapsula* sp. cf. *S. palmerae* Pessagno, 10GR34. 21) *Tethysetta* sp. cf. *T. mashitaensis* (Mizutani), 10GR34.